Circulation Research

REVIEW

Cardiac Tissues From Stem Cells

New Routes to Maturation and Cardiac Regeneration

Giulia Campostrini,* Laura M. Windt,* Berend J. van Meer, Milena Bellin, Christine L. Mummery

ABSTRACT: The ability of human pluripotent stem cells to form all cells of the body has provided many opportunities to study disease and produce cells that can be used for therapy in regenerative medicine. Even though beating cardiomyocytes were among the first cell types to be differentiated from human pluripotent stem cell, cardiac applications have advanced more slowly than those, for example, for the brain, eye, and pancreas. This is, in part, because simple 2-dimensional human pluripotent stem cell cardiomyocyte cultures appear to need crucial functional cues normally present in the 3-dimensional heart structure. Recent tissue engineering approaches combined with new insights into the dialogue between noncardiomyocytes and cardiomyocytes have addressed and provided solutions to issues such as cardiomyocyte immaturity and inability to recapitulate adult heart values for features like contraction force, electrophysiology, or metabolism. Three-dimensional bioengineered heart tissues are thus poised to contribute significantly to disease modeling, drug discovery, and safety pharmacology, as well as provide new modalities for heart repair. Here, we review the current status of 3-dimensional engineered heart tissues.

Key Words: cardiac tissue ■ drug discovery ■ heart failure ■ humans ■ stem cells

Downloaded from http://ahajournals.org by on March 22, 2021

In 1998, James Thomson described the derivation of pluripotent human embryonic stem cells (hESC). It was only a matter of time before beating cardiomyocytes were identified in differentiating cultures and inevitable that human induced pluripotent stem cells (hiPSCs), derived around 10 years later,[1] also differentiated to beating cardiomyocytes. Studies using healthy or patient-derived hiPSC cardiomyocytes for transplantation to repair the heart after damage and in vitro disease modeling were rapidly initiated. Channelopathies caused by mutations in cardiac ion channels were most abundantly studied[2] and cell transplantation advanced,[3] but immaturity of hiPSC cardiomyocytes has remained an obstacle: they fall short in mimicking the biological and physiological phenotype of cardiomyocytes in the 3-dimensional (3D) heart in vivo. Recent evidence shows that cardiac tissue engineering may address this and thus accelerate use of hiPSC in preclinical drug testing, identifying mechanisms underlying genetic and acquired human heart disease and in cardiac regeneration therapy. Here, we present the latest engineered models based on cardiac derivatives of human pluripotent stem cells (hPSCs) and discuss their applications in human heart research.

WHY DO WE NEED 3D CARDIAC MODELS?

Models to study any question are ideally as simple as possible and as complex as necessary. In that sense, there would be no need to increase the complexity of current heart models if simpler models—2-dimensional (2D) cardiomyocytes or noncardiomyocytes expressing cardiac genes ectopically—reflected physiology in vivo or predicted drug responses accurately. Simple models are often easier to implement than their 3D counterparts. For example, single-cell patch-clamp electrophysiology in substrate-attached cardiomyocytes is still the gold standard to quantify parameters such as upstroke velocity, membrane potential, and ion currents. Similarly, voltage-sensitive dyes and multielectrode arrays were developed for use in 2D monolayer cultures. These simple models

Correspondence to: Christine L. Mummery, PhD, Department of Anatomy and Embryology, Leiden University Medical Center, Einthovenweg 20, 2333 ZC Leiden, the Netherlands. Email c.l.mummery@lumc.nl

*G. Campostrini and L.M. Windt contributed equally.

For Sources of Funding and Disclosures, see page 795.

© 2021 American Heart Association, Inc.

Circulation Research is available at www.ahajournals.org/journal/res

REVIEW

Nonstandard Abbreviations and Acronyms

2D	2 dimensional
3D	3 dimensional
ACM	arrhythmogenic cardiomyopathy
CF	cardiac fibroblast
CV	conduction velocity
CW	cardiac wire
EC	endothelial cell
ECM	extracellular matrix
EHM	engineered human myocardium
EHT	engineered heart tissue
FFR	force-frequency relationship
hESC	human embryonic stem cell
hiPSC	human induced pluripotent stem cell
hPSC	human pluripotent stem cell
MI	myocardial infarction
MTF	muscle thin film
PDMS	polydimethylsiloxane
PS	polystyrene
PRP	post-rest potentiation

have been widely used to detect disease and drug effects in hPSC cardiomyocytes and even though highly reductionist versions of the real heart, they often reproduce responses of native tissue. Examples include ion channel mutations causing long QT syndrome (eg, mutations in *KCNQ1*),[4] Brugada syndrome (mutations in *SCN5A*),[5] and catecholaminergic polymorphic ventricular tachycardia (mutations in *RYR2*).[6] In addition, drug-induced changes in electrophysiology[7–10] or contractility[11–13] or combinations of both[14] in 2D hPSC cardiomyocytes have been shown to predict toxic effects on the heart accurately, in some cases better than standard animal models.

Not uncommonly, however, single-cell or 2D models fail to capture expected phenotypes. Typically, this is the case for genetic defects that impair structural proteins, such as myosin-binding protein C or desmosomes, associated with hypertrophic cardiomyopathy and arrhythmogenic cardiomyopathy (ACM), respectively. While phenotypes have been revealed in hPSC cardiomyocytes cultured in media that promote maturation in single-cell and 2D formats in the case of hypertrophic cardiomyopathy,[15] ACM required not only structural and metabolic maturation but also stress conditions, complex 3D models,[16–19] and noncardiomyocyte populations.[20] Similarly, for mutations in *TTN*, the gene encoding the large sarcomere protein titin causing dilated cardiomyopathy, contractility in hiPSC cardiomyocytes was unchanged in 2D while it was impaired in 3D. Enhanced hPSC cardiomyocyte maturation in 3D may be one reason for this, besides more physiological load on the cardiomyocytes. Load directly changes the output force and work that cardiomyocytes need to deliver[21]; this might enhance maturation. For drug-induced changes in electrophysiology or contractility, immaturity might explain why certain drug classes such as PDE3 (phosphodiesterase enzyme 3) inhibitors do not affect single-cell or 2D hPSC cardiomyocytes (which do not express PDE3A) while 3D hPSC cardiomyocytes (expressing PDE3[20]) respond as expected.[22]

While considerable effort has been made to develop highly efficient differentiation protocols and enrich for hPSC cardiomyocytes in differentiating hPSC cultures, noncardiomyocytes increase both contractility and electrophysiology, so that in recent studies, cardiomyocytes are often no longer purified or noncardiomyocytes are added before creating 3D tissues. Coculture conditions are still being optimized: for example, addition of cardiac fibroblasts (CFs) promotes cellular organization, but high CF:cardiomyocyte ratios in a cardiac tissue can cause conduction blocks, increase stiffness, and slow down conduction.[23] Correct substrate stiffness[24] and medium components[25] are essential for physiologically relevant cardiac responses.

For more complex cardiac disease, it may be important to include inflammation and reduce oxygen (hypoxia) as in myocardial infarction (MI) or mimic fibrosis that follows heart damage. Adding inflammatory components (eg, macrophages and inflammatory proteins) or vascularization requires more advanced 3D models. These are models in which cells can grow or move in the 3D space. In the following sections, we discuss what they have contributed to the field so far.

3D CARDIAC MODELS

Scaffold-Free Cardiac Tissues

Scaffold-free cardiac tissues, in whatever form or combination of cell types, are self-organizing structures in which there is cross-talk between cells; they position within structures and deposit their own ECM (extracellular matrix). They fall broadly into 3 categories (Figure 1): cardiac microtissues, 3D-bioprinted tissues, and cardiac cell sheets. A hybrid variant, where a mixture of hiPSC cardiomyocytes and fibroblasts anchored to the substrate in a dog bone shape that allows uniaxial stress on the 3D tissue, has also been reported.[26]

3D Cardiac Microtissues

Cardiac microtissues are spheroids of heart cells usually formed by self-aggregation. The process is rapid and generally does not require specific equipment. Direct cell-cell contacts and paracrine cell communication take place within the spheroids, followed by ECM deposition and interaction in the tissue microenvironment, much as in normal heart development. Cardiac microtissues from hPSCs are similar to hPSCs differentiated in aggregates called embryoid bodies, except that the cardiac input cells are predifferentiated, whereas in embryoid bodies,

Downloaded from http://ahajournals.org by on March 22, 2021

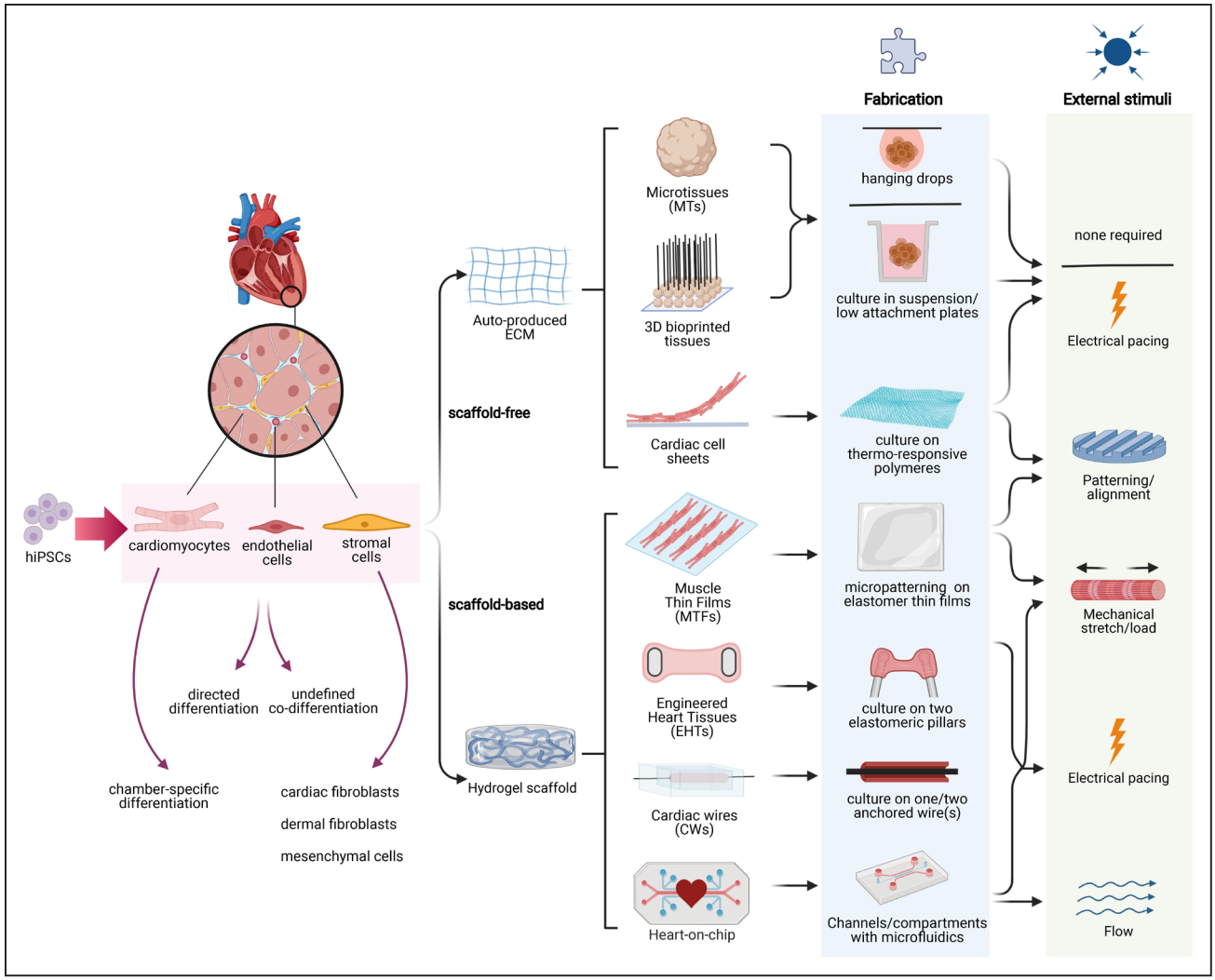

Figure 1. Three-dimensional (3D) cardiac models.
Overview of scaffold-free and scaffold-based 3D cardiac models. **Left**, The main cardiac cell types (cardiomyocytes, endothelial cells, and stromal cells) included in multicell type 3D cardiac models and can be derived either from primary (animal) tissue or from human induced pluripotent stem cells (hiPSCs). **Right**, Fabrication methods and external stimuli for each type of cardiac model are shown schematically. CW indicates cardiac wire; ECM, extracellular matrix; EHT, engineered heart tissue; MT, microtissue; and MTF, muscle thin film.

differentiation is directed by growth factor addition or is spontaneous, so that derivatives of germ layers other than mesoderm may be present.[27] Cardiac microtissues can be formed from small cell numbers and are usually <300 µm in diameter so that oxygen and nutrients reach the center of the tissue.[28,29] Aggregation itself is facilitated by suspending cells in hanging drops,[30–32] in rotating suspension cultures for 2 days,[33,34] culture in nonadhesive agarose hydrogel molds,[35] or most commonly in low-attachment plates.[11,20,36–40] Early studies using primary neonatal rat cardiomyocytes showed self-aggregation in 3D, spontaneous and synchronous beating, ECM production, and retention of cardiomyocyte properties.[41,42] Addition of endothelial cells (ECs) to these microtissues resulted in vascular-like structures forming and inclusion of fibroblasts improved cell viability, self-organization, and contractile function.[36,43] Similar results were obtained using hPSC cardiomyocytes in microtissues containing ECs or fibroblasts, or both. Input ratios of the different cell types in microtissues can be controlled and optimized to recapitulate the cellular composition of the human fetal or adult heart (either in cell number or occupied volume). Ratios reflecting those in the fetal heart, where there are twice as many cardiomyocytes to noncardiomyocytes than in adult heart, enhanced microtissue contraction, structure, and function[35] although other studies using different ratios showed similar effects (Tables 1 and 2).

Because they are easy to fabricate, amenable to high-throughput imaging and cell viability assessment, and their contractility is not dictated by physical properties of the substrate, cardiac microtissues are being used to investigate structural cardiotoxicity of drugs not only directly on cardiomyocytes, but also indirectly via the noncardiomyocytes also present.[44] Cardiac microtissues have also been used as models to study MI: cell viability decreased in microtissues following hypoxia (10% O_2), accompanied

Downloaded from http://ahajournals.org by on March 22, 2021

REVIEW

Table 1. Composition, Structure, Gene Expression, and Metabolism of 3D Cardiac Tissues

3D model	Reference	Cell types present	Pacing/ stretching regime	Structure				Gene expression	Metabolism	Serum free
				Cell numbers and size	ECM	CM morphology	Sarcomere length and alignment			
MTs	33	hESC-CMs		1–12×10^6 cells; d, 2–10 mm	Free		Increased myofibrillar organization	Increased expression of *Nkx2.5* and *β-MHC* with time in culture		Yes
MTs	34	hESC-ECs:HUVEC stromal:NHDFs (1:1:0.5)		3×10^6 cells	Free					Yes
MTs	37	hESC-CMs:fetal CFs:primary hCMECs (4:2:1)		1000 cells; d, ≈250–300 µm	Free			Upregulation of *S100A1*, *TCAP*, *PD3A*, *NOS3*, *ADRB1*, *KCND3*, *MYH6*, and *MYH7*		No
MTs	38	hiPSC-CM:hiPSC-ECs (85%:15%)		5000 cells; d, ≈250–300 µm	Free			Upregulation of mature isoform of SC proteins, ion channels, Ca^{2+}handling genes		Yes
MTs	35	hiPSC-CMs:CFs:HUVECs (5:4:1)		150 000 cells	Free		Improved SCs in Z-line width (n.q.)	Upregulation of *MLC2v* and *cTnTI*, increased ratios *TNNI3*/*TNNI1*, and *MYL2*/*MYL7*		No
MTs	30	hiPSC-CMs:ECs:hiPSC-CFs (2:1:1)		10 000 cells; d, ≈400 µm	Free					Yes
MTs	11	hiPSC-CMs:CF:hCMEC (4:2:1)		500 cells; 48 524 µm^2±5074	Free					No
MTs	39	hiPSC-CMs:CFs (90%:10%)		1000 cells; d, ≈250 µm	Free					Yes
MTs	40	hiPSC-CMs		1500 cells; d, ≈200 µm	Free			Upregulation of CM specification and maturation genes (SC proteins, ECM, and oxidative metabolism)	Reduced glycolysis, increased oxidative decarboxylation of pyruvate and ATP production	Yes
MTs	20	hiPSC-CM:hiPSC-EC:hiPSC-CFs (70%:15%:15%)		5000 cells; d, ≈400 µm	Free		≈1.7–1.9 µm, increased (≈0.025 alignment index)	scRNAseq and bulk RNAseq: increased SC proteins, upregulation of genes associated with heart contraction, cardiac conduction, membrane potential, ion channels, adrenergic signaling	Increased mitochondrial respiration	Yes
MTs	31	hiPSC-CMs:embryonic CFs (80%:20%)		5000 cells; d, ≈400 µm	Free			Increased *ACTN2* and *TNNI3*/*TNNI1* ratio		Yes
3D bioprinted MTs	53	hiPSC-CMs:hCFs:HUVECs (70%:15%:15%)		33 000 cells; 500–550 µm per MT	Free, 3D bioprinted onto needle array					Yes
3D bioprinted MTs	54,55	iCells:HUVECs:NHDFs (50%:25%:25%)		35 000 cells; ≈600 µm per MT	Free, 3D bioprinted					Yes
Cell sheets	142	hiPSC-CMs		43 200 cells; 144 cm^2	Free (cell sheet)+fibrin gel					No
EHT	25	hESC-CMs and hiPSC-CMs (plus co-differentiated stromal cells, epicardial cells, FBs, ECs)		5×10^4 cells, ≈1.3×0.5 mm, 3.5 µL	Collagen I, Matrigel		≈2.3 µm, highly organized Z and I bands, intercalated discs (n.q.)	Upregulation of cardiac developmental genes, metabolic switch, DNA damage, reduced cell cycle activity	Pre- to postnatal switch in metabolic substrates from carbohydrates to fatty acids (well-developed mitochondria)	No

(*Continued*)

Downloaded from http://ahajournals.org by on March 22, 2021

Table 1. Continued

3D model	Reference	Cell types present	Pacing/ stretching regime	Structure				Gene expression	Metabolism	Serum free
				Cell numbers and size	ECM	CM morphology	Sarcomere length and alignment			
EHT	139,141	hiPSC-CM	0.5 Hz for 2 wk or week 1: 2 Hz/wk 2: 1.5 Hz	1×10^6 cells, ≈10×2 mm	Fibrin, Matrigel (100uL: 10uL)	rod shaped	CMs aligned, Z disks, M bands (n.q.)			No
EHT	80	hESC-CMs		0.6×10^6 cells, ≈8×0.75 mm, 100 μL	Fibrin		≈6.2% improved SC organization and alignment compared with control, longitudinally oriented	*β-MHC* expression upregulated 2- to 3-fold		No
EHT	126	hiPSC-CMs:human dermal FBs (75%:25%)	Control (no stimulation), constant (3 wk at 2 Hz), intensity training (2 wk at increasing rates 2–6 Hz by 0.33 Hz/day, then 1 wk at 2 Hz)	2×10^6 cells, ≈6×1.8 mm, 200 μL	Fibrin	Elongated (elongation ratio ±0.75), rod shaped	≈2.2 μm, SCs with I/A bands, M lines, Z lines, desmosomes, intercalated discs (n.q.)	Upregulation of adult-like conduction maturation, ultrastructure, energetics, Ca^{2+} handling	Oxidative metabolism, phospholipid production near sarcomeres (percentage area mitochondria in cells ≈30%)	No
EHT	87	hiPSC-CMs		1×10^6 cells	Fibrin, Matrigel		≈1.6 μm, aligned SCs, regular Z lines, inconsistent I- and A-band formation (n.q.)	*MLC2a–/MLC2v+* CM population in the EHT format		No
EHT	82	hiPSC-CMs	2 wk: control/static stress 125%/static stress 125%+2 Hz (1 wk)	2×10^6 cells, 20×1×0.3 mm, 100 μL	Collagen I	Increased	Myofibrillar alignment, Z lines (n.q.)	*RYR2* increased		Yes
CW	23,102	hESC-CMs/ hiPSC-CMs:CFs (75%:25%)		1×10^5 cells, 5 mm×1 mm×300 μm	Collagen/ Matrigel, collagen/fibrin	Larger than age-matched CMs from EBs	Alignment ratio ±0.7, organized banding, frequent converging myofibrils, aligned Z discs, more H zones and I bands	Increased *TTN N2B*, *MYH7/6*, *TNNI3/1*; downregulated *NPPA*, *NPPB*, *MYH6*, *MYH7*, *IRX4*, *MYBPC3*		No
EHT	100,147	hESC-CMs/ hiPSC-CMs:human foreskin FBs (90%:10%)	Stepwise increase in static stretch, up to ≈125%	5×10^5 cells, 6 mm, 220 μL	Collagen I, Matrigel		≈1.75 μm, improved organization, intercalated discs, enhanced alignment, Z bands and H bands (n.q.)	Maturation genes upregulated		No
EHM	107	hESC-CMs/hiPSC-CMs:human FBs (75%:25%)	Passive stretch: 5, 7, or 9 mm	1.6×10^6 cells, ≈3×5/7/9 mm, 100 μL	Collagen I, Matrigel		Cell alignment (n.q.)	Maturation genes upregulated: β-adrenergic receptors 1 and 2, calveolin-3, K^+ and Ca^{2+} ion channels, troponin-T		No
EHM	89	hESC-CMs/hiPSC-CMs:ECs:HUVEC stromal cells (MSC) or mouse embryonic FBs (50%:25%:25%)	No stress, static stress, and 1 Hz cyclic stress conditioning for 4 d	2×10^6 CMs+1×10^6 HUVEC+1×10^6 MSCs/MEFs, 20×3 mm, 100 μL	Collagen I	Increased (under mechanical stress)	More aligned under static and cyclic stress, partially organized myofilament bundles, nascent Z lines (n.q.)	*BMHC* expressed		No

(*Continued*)

Downloaded from http://ahajournals.org by on March 22, 2021

Table 1. Continued

3D model	Reference	Cell types present	Pacing/ stretching regime	Structure				Gene expression	Metabolism	Serum free
				Cell numbers and size	ECM	CM morphology	Sarcomere length and alignment			
EHT	85	hESC-CMs/ hiPSC-CMs: skin FBs, gingiva- and heart-derived FBs (70%:30%)		1.5×10^6 cells, ≈0.5×0.5×6 mm	Collagen I, Matrigel	Elongated, rod shaped	≈1.93 μm, Z, I, A, H, and M bands, more SC protein per CM (n.q.)	Advanced molecular maturation by transcriptome profiling		Yes
EHT rings	136	hiPSC-CM		4×10^5 cells, 432.72± 56.18 μm			≈1.83 μm, improved organization, larger SC bundles, well-defined Z disks, A bands, and myofibrils (n.q.)	Maturation genes upregulated		After day 2
EHT rings	137	hESC-CM (atrial and ventricular)	Steps of 0.2 mm stretch up to 1.2 mm	2×10^6 cells, ≈0.5×0.5×6 mm	Collagen					No
HoC	110,111	hiPSC-CMs (plus co-differentiated: cardiac stromal cells) (78.5%:20.4%)	Mechanical stretching of 10%, 1 Hz (2 d)	4.5×10^4 cells, 100×50× 300 μm	Fibrin	Rod shaped	More complex organization, intercalated discs, gap junctions (n.q.)			No
HoC	109	hESC-CM, human dermal FBs (90%:10%)	Pressure load controlled with an adjustable hydrostatic fluid column	1×10^7 cells; wall thickness, ≈100 μm; diameter, ≈1.3 cm	Collagen I, Matrigel		≈1.6 μm, more complex organization, Z lines, myofibrils intercalated with mitochondria	Increased: *PLN* and *RYR*, ion channel *KCNJ2*, *MYH6* and *MYH7*, *CX43*		No
HoC	149	hESC-CM and hiPSC-CM	Static or dynamic culture conditions (rocking 30-degree tilt, 0.4 Hz)	3.75×10^5 cells, 7×2 mm	Fibrin	Increased ≈2.1-fold	Improved sarcomere alignment (n.q.)			No

3D indicates 3 dimensional; CF, cardiac fibroblast; CM, cardiomyocyte; CW, cardiac wire; CX43, connexin 43; EB, embryoid body; EC, endothelial cell; ECM, extracellular matrix; EHM, engineered human myocardium; EHT, engineered heart tissue; FB, fibroblast; hCMEC, human microvascular endothelial cell; hESC, human embryonic stem cell; hiPSC, human induced pluripotent stem cell; HoC, heart-on-chip; HUVEC, human umbilical vein endothelial cells; MEF, mouse embryonic fibroblasts; MSC, mesenchymal stem cells; MT, microtissue; n.q., not quantified; NHDF, neonatal human dermal fibroblast; RNAseq, RNA sequencing; SC, sarcomere; and scRNAseq, single-cell RNA sequencing.

by sarcomere and mitochondria disorganization and altered secretion of cytokines, which recovered during the postischemia to postreperfusion transition.[45] Three cell type microtissues exposed to hypoxia in another study showed an outside-to-inside oxygen gradient causing the center of the spheroid to become apoptotic, again mimicking MI. This was accompanied by differential gene expression, impaired oxidative metabolism with increased fibrosis that led to aberrant calcium (Ca^{2+}) handling, similar to that in the native human heart after MI. Of note, the effect on Ca^{2+} handling was not observed in microtissues without fibroblasts.[46] We recently used 3-cell type microtissues to model ACM—a rare genetic cardiac disease characterized by arrhythmia followed by formation of fibrofatty deposits. Inclusion of hiPSC CFs from ACM patients in cardiac microtissues was sufficient to induce arrhythmia during pacing, even when the hiPSC cardiomyocytes and ECs in the microtissues were from healthy controls. CX43 (connexin 43) gap junction expression was decreased in the microtissues, suggesting that defective cardiomyocyte-CF communication could contribute to arrhythmia in ACM patients.[20]

3D Bioprinted Cardiac Tissues

3D bioprinting using bioink composed of cardiac cells (and hydrogels) can be used to produce larger cardiac tissues, rapidly and in large numbers. The challenge, however, is to minimize cell stress during printing and provide close-to-native cardiac ECM.[47] Bioprinting methods have recently been reviewed[48–51] but in essence started using rat or hiPSC cardiomyocytes with hydrogel bioinks made from collagen, alginate, gelatin, or fibrin printed in the form of cardiac patches.[50,51] Scaffold-free bioprinting is also feasible and provides better biocompatibility for transplantation to the heart. Bioprinting has the advantage over microtissues that complex tissue architectures with specific cell organization can be created. Although cells for bioprinting can be added to

Downloaded from http://ahajournals.org by on March 22, 2021

the construct individually, most often they are first preassembled as microtissues so that they produce their own ECM giving the construct greater stability. This method is faster than single-cell and hydrogel printing, but ECM production can be insufficient or variable.[52] For the first bioprinted microtissues with hiPSC cardiomyocytes, ECs, and fibroblasts together, vacuum suction was used to load individual preassembled microtissues containing 33 000 cells onto a needle array, such that they overlapped and fused, forming a large, scaffold-free tissue. The constructs engrafted and were vascularized after implantation in nude rat hearts.[53] Tubular scaffold-free constructs have also been built in a similar way using multiple layers of 3-cell type microtissues[54]; these were sensitive to isoproterenol and propranolol and toxic effects of doxorubicin.[55] Microtissues can also be printed layer by layer, which is especially useful for transplantation in vivo when larger constructs are required.[56]

Overall, 3D printing still requires the needle array, which acts as a support much like scaffold material; this increases prefabrication time and costs, and moreover, interactions of cells with the needle may interfere with cell-cell and cell-ECM interactions.

Cardiac Cell Sheets

3D cardiac cell sheets have been produced mainly for heart regeneration, since they preserve native ECM-cell interaction by omitting scaffolds. Cells can be detached as sheets from the culture dishes without use of enzymes by precoating the substrate with a temperature-responsive polymer, to which cells adhere at 37 °C but not at room temperature (20 °C). These sheets are then combined into multiple layers for direct use or transplantation into the heart.[57,58] When thermoresponsive cell culture dishes coated with poly(N-isopropylacrylamide)[59] were used to produce 3D cardiac tissues from rat cardiomyocytes, the sheets beat synchronously after detachment, established gap junction connections, and became electrically active and coupled with adjacent sheets.[57,60,61] Elongated sarcomeres were observed in these tissues after transplantation into the subcutaneous space or hearts of nude rats.[62,63]

Scaffold-Based Tissues

3D cardiac tissues have also been developed that deposit cells in scaffolds (Figure 1). These custom-designed biomimetic scaffolds recapitulate the geometric boundary conditions seen in vivo and thus guide cell self-organization into more physiologically relevant architectures. In the native heart, preload is the stretch during chamber filling, while afterload is the pressure the heart must work against to eject blood; these can be mimicked by anchoring or stretching the tissues, respectively. Indeed, tissues can contract unidirectionally against a load determined by scaffold properties (material stiffness or the presence of fixed attachment points like pillars). The scaffold properties can be used to calculate the force generated by the cardiac tissues by (1) measuring the displacement of points to which the scaffold is attached, (2) calculating the force required for the displacement knowing the material properties, and (3) dividing this force by the cross section of the tissue to obtain force per square micrometer. Scaffold mechanical and structural support maximize the viability of cardiomyocytes, which align in the direction of contraction. Various hydrogel mixtures have been used (collagen, Matrigel, and fibrin proteins); all can affect cell migration, organization, and functionality by engaging different cell surface integrins (ECM receptors) or having variable shear moduli. Engineered tissues have been formed in 2D or 3D formats as muscle thin films (MTFs), cardiac wires (CWs) or engineered heart tissues (EHTs) (Figure 1). We consider each of these individually below.

Muscular Thin Films

MTFs enable topological control of cardiomyocyte cultures as the cells are plated on elastomer thin films micropatterned with ECM proteins. The ECM patterns are typically arrays of lines with widths ≈15 to 115 μm and spaces between the lines ≈20 to 25 μm. The cardiomyocytes align and form anisotropic monolayers,[64–66] which facilitate synchronized contraction, and because the MTF is fixed at one end, it curls up during systole and flattens during diastole[66]; this displacement can be measured using high-speed, high-resolution imaging, and knowing the material properties and geometry, the force generated can be calculated.[67] MTFs are usually made of polydimethylsiloxane (PDMS) using microfabrication techniques. The load on the cardiomyocytes can be altered by changing the substrate thickness.[67,68] Microfabrication allows actuators, electrodes, and force sensors[69] to be embedded in the MTF, enabling, for example, electrical field stimulation of the tissue.[70] Microcontact printing can be used to deposit ECM proteins in any geometric pattern on PDMS, with cardiomyocytes adopting the same shape as the patterned matrix. First, MTFs used rat cardiomyocytes,[71] but later, hiPSC cardiomyocytes were used.[72] Of note, neonatal rat cardiomyocytes remodeled shape and cytoskeleton within 48 hours, faster than adult cardiomyocytes,[73] but remain functional for weeks.[72] Two studies used MTFs to model mitochondrial cardiomyopathy[74] and catecholaminergic polymorphic ventricular tachycardia[75] and found that reactive oxygen species scavenging might benefit Barth syndrome patients and abnormal calmodulin-dependent protein kinase II–dependent reentry plays a role in catecholaminergic polymorphic ventricular tachycardia. Apart from standard multiwell plate formats, MTFs can also be included in 3D microphysiological system environments such as a fluidic channel or an endothelial barrier insert.[70,76,77]

Downloaded from http://ahajournals.org by on March 22, 2021

Table 2. Electrophysiology, Ca^{2+} Handling, and Contractility in 3D Cardiac Tissues

3D model	Reference	Electrophysiology						Ca^{2+} handling
		Spontaneous beating	Type of analysis	V_{max}, RMP, APA	APD	CV	Ion channels/ regulators and gap junctions	Ca^{2+} transients
MTs	33	Yes						Yes, synchronous, n.q.
MTs	34	Yes						
MTs	37	Yes, 54±5 bpm						Yes, amplitude ≈4 nm
MTs	38	Yes, ≈12 bpm						
MTs	35	Yes						Yes, n.q.
MTs	30	Yes						
MTs	11	Yes, 62±24 bpm						
MTs	39	Yes, 30 bpm						
MTs	40	Yes, 57.9±1.8 bpm	Optical	V_{max} increased compared with 2D culture	APD_{90}, ≈450; APD_{50}, ≈350			
MTs	20	Yes, ≈20 bpm	Single-cell and sharp-electrode p.c.	In dissociated cells, V_{max}, 150 V/s; RMP, −70 mV; APA, 100 mV	Single cells: APD_{90}, ≈250 ms		Increased expression of ion channels, gap junctions between CMs and CFs	Yes, increased time to peak and decreased decay time
MTs	31	Yes, ≈90 bpm	Sharp-electrode p.c.	V_{max}, <10 V/s; RMP, −41 mV; APA, 66 mV	APD_{90}, ≈500 ms			Yes, regular
3D bioprinted MTs	53	Yes	Optical mapping		Under 0.5–16 Hz pacing: APD_{30}, 140–180 ms; APD_{80}, 210–250 ms	1.8–3 cm/s with 0.5–1.6 Hz pacing	CX43 expression at the cell-cell borders	
3D bioprinted MTs	54,55	Yes, ≈12 bpm (2018), ≈60 bpm entire tissue (2020)						
Cell sheets	142	Yes						Yes, synchronized
EHT	25	Yes, 31±1 bpm	Whole-cell p.c.	V_{max}, 4.7±0.7 F/F0/s; RMP, −79±0.4 mV; APA, ≈120 mV	APD_{50}, ≈0.06±0.01 s; APD_{90}, ≈0.11±0.02 s		CX43, pancadherin	Increased peak amplitude, rising slope, and decay
EHT	139,141	Yes, ±60 bpm	Sharp-electrode p.c.	V_{max}, 219±15 V/s; RMP, −73.5 mV; APA, ≈102.7 mV			CX43	
EHT	80	Yes, 40–70 bpm	Zero current p.c.	V_{max}, 10.4±1.2 V/s; RMP, 49±1.2 mV; APA, 85±2.8 mV	APD, 260–1200 ms; APD_{80}, 887±71 ms		CX43	
EHT	126	Yes, 125 bpm	Whole-cell p.c.	V_{max}, ≈23 V/s; RMP, −70±2.7 mV; APA, ≈45 mV	APD_{50}, ±300-400 ms; APD_{90}, ±600–750 ms	25±0.9 cm/s	CX43, intercalated discs, desmosomes, I_{K1} current (peak inward density of −9.9±3.8 pA/pF; peak outward density of 0.30±0.12 pA/pF)	Increased

(*Continued*)

Downloaded from http://ahajournals.org by on March 22, 2021

Table 2. Continued

Ca^{2+} handling		Contractility					
Ca storage and SR release	T-tubule development	Contraction kinetics	MCR	Maximum active force	Frank-Starling relationship	Force-frequency relationship	Inotropic response to compounds
			Up to 2–3 Hz	7.9±3.1 mN/mm^2	Yes		
			Up to 3 Hz				Yes
							Yes
							Yes
			Up to 3 Hz				
							Yes
		Contraction velocity ≈0.09 µm/ms					
	T tubule–like structures at electron microscopy	Contraction rate, duration, and amplitude increased, higher contraction and relaxation velocity	Up to 3 Hz				
		Decreased contraction rate, no difference in other parameters	Up to 4 Hz				
		Contraction amplitude increased compared with 2-cell type tissues	Up to 2 Hz				Yes
				3.3±0.6 mN/mm^2	Yes	No	Yes, on force and beating rate
More mature, increased Ca^{2+} EC50, in MM higher Ca^{2+} EC50 for contraction force (1.0 mmol/L Ca^{2+}) than in control medium (0.3 mmol/L Ca^{2+})	Yes (cav-3 immunostaining)			≈300 µN		Positive	Yes, isoproterenol, Ca^{2+}
I_{Na} density (−18.5±1.9 pA/pF)		Time to peak, 0.181±0.004 s; time of decay, 0.329±0.003 s		≈165 µN		Positive	Yes, isoproterenol (+51%)
				≈100 µN/0.12 mN/mm^2			Yes, isoproterenol, but not significant
Functional Ca^{2+} handling, FDAR	Yes	Time to peak, ≈50–100 ms; time of decay, ≈200–350 ms	Up to 6 Hz	≈3 mN/mm^2 (6 Hz), ±2.5 mN/mm^2 (1 Hz)		Positive	Yes, isoproterenol

(*Continued*)

Downloaded from http://ahajournals.org by on March 22, 2021

Table 2. Continued

3D model	Reference	Electrophysiology					Ca^{2+} handling	
		Spontaneous beating	Type of analysis	V_{max}, RMP, APA	APD	CV	Ion channels/ regulators and gap junctions	Ca^{2+} transients
EHT	87	Yes, 61±2 bpm						
EHT	82	Yes						
CW	23,102	Yes (30%), nonbeating (70%)	Sharp-electrode p.c.	V_{max}, ≈20 V/s; RMP, ≈—60 to 70 mV; APA, ≈70 mV	APD_{30}, ±20 ms; APD_{50}, 50 ms; APD_{90}, 100 ms	≈±15 cm/s, up to ≈50% higher (6 Hz ramp up)	CX43, more desmosomes per membrane length, some nascent intercalated discs	Electrically stimulated cells had greater response to caffeine than nonstimulated controls
EHT	100,147	Yes, 54.4±3.6 bpm		APA, ≈50 mV		4.9 cm/s	CX43, titin collagen fiber alignment	
EHM	107	Yes, ≈10–70 bpm						
EHM	89	Yes, 0.71–0.95 Hz						
EHT	85	Yes	Sharp-electrode p.c.	V_{max}, 45±5 V/s; RMP, −57±2 mV; APA, 97±2 mV	APD_{20}, 234±10 ms; APD_{50}, 389±10 ms; APD_{90}, 436±22 ms		Presence of N-cadherin and intercalated disc-like structures	
EHT rings	136	Yes, 0.2–4 Hz						
EHT rings	137	Yes	Whole-cell p.c.	RMP, ≈—60 mV	Ventricular vs atrial tissue constructs: APD_{90}, 420±11 vs 230±5 ms; APD_{50}, 254±8 vs 152±4 ms; APD_{30}, 190±7 vs 118±3 ms	21.4±4.4 cm/s	CX43	
HoC	110,111	Yes		APA higher in stimulated tissues			CX43, N-cadherin	
HoC	109	Yes, 0.76±0.06 Hz			APD_{50}, ≈340 ms; APD_{90}, ≈550 ms	≈6 cm/s	Desmosomes and gap junctions	
HoC	149	Yes but stopped after 10 days				25.8 cm/s	Electrical and mechanical junctions	1.6-fold increase in Ca^{2+} transient amplitude

(*Continued*)

Downloaded from http://ahajournals.org by on March 22, 2021

Table 2. Continued

Ca^{2+} handling			Contractility				
Ca storage and SR release	T-tubule development	Contraction kinetics	MCR	Maximum active force	Frank-Starling relationship	Force-frequency relationship	Inotropic response to compound
Small PRP suggests SR is underdeveloped but functional	Immature T-tubule formation	Time of decay, 0.163±0.003 s, contraction time, 0.120±0.002 s	Up to 2 Hz	≈152 μN	Yes	Neutral	Yes, isoproterenol, Ca^{2+}, ouabain, Bay K-8644, EMD-57033, rolipram, ryanodine, verapamil
				≈1.34±0.19 mN/mm^2	Yes	Negative	Yes, L-type Ca^{2+} channel agonist Bay K-8644
Yes, I_{Kr} currents were larger (~0.8 pA/pF) and I_{K1} densities higher (~1.5 pA/pF)	No	Time to peak, 0.069±0.005 ms; time of decay, 0.419±0.043 s	±3.8 Hz	±12 (1 Hz), 14 (2 Hz), 16 uN (3 Hz) (after 42 d)		Positive	Yes
		Time to peak, 80 ms	Up to 5 Hz	≈1.37+0.18 mN (d21), 4.4 mN/mm^2	Yes	Positive	Yes, isoproterenol
Upregulation of β-adrenergic receptor 1, expression of β-adrenergic receptor 2 unchanged, indicating maturation	Increased t-tubule protein cav-3 expression	Time to peak, ≈300 ms (1 Hz)		≈500 μN			
				≈500 μN, 0.08 mN/mm^2, passive force up to 0.4 mN/mm^2 while stretching to 170%	Yes		
Yes, PRP observed (+9±1% contraction force in the first electrically stimulated beat after a stimulation pause)			Up to 3 Hz	6.2±0.8 mN/mm^2, at 1.5 Hz	Yes	Positive: +19±5% at 2 Hz, +22±6% at 3 Hz vs 1 Hz, studied at 4 wk	Yes, isoproterenol, Ca^{2+}
Greater maturation in Ca^{2+}-handling properties			Up to 4 Hz	0.54±0.15 mN/mm^2	Yes		
Increased contraction following elevation of extracellular Ca^{2+}	Lack of t tubules			≈2 mN/mm	Yes		Yes, isoproterenol
			≈5.7 Hz				
			Up to 3 Hz		Yes	Negative	Yes, isoproterenol
				≈1.3±0.051 mN	Yes		

2D indicates 2 dimensional; 3D, 3 dimensional; APA, action potential amplitude; APD, action potential duration; bpm, beats per minute; cav-3, caveolin-3; CF, cardiac fibroblast; CM, cardiomyocyte; CV, conduction velocity; CW, cardiac wire; CX43, connexin 43; EC50, half maximal effective; concentration; CX43, connexin 43; EHM, engineered human myocardium; EHT, engineered heart tissue; FDAR, frequency-dependent acceleration of relaxation; HoC, heart-on-chip; MCR, Maximum capture rate; MM, maturation medium; MT, microtissue; n.q., not quantified; p.c., patch clamp; PRP, post-rest potentiation; RMP, resting membrane potential; SR, sarcoplasmic reticulum; and V_{max}, maximal upstroke velocity.

Downloaded from http://ahajournals.org by on March 22, 2021

Engineered Heart Tissues

EHTs were first developed using neonatal or embryonic cardiomyocytes from rat or chicken heart.[78,79] EHTs based on hydrogels, containing cardiac cells cast in a mold with 2 elastomeric pillars, are now widely used. The cells self-organize as the hydrogel compacts and forms a tissue bundle around the two pillars, which exert continuous mechanical strain promoting cell alignment and thus auxotonic contraction of the tissue. From pillar deflection, optical readouts of contractile parameters (frequency and contraction and relaxation times) can be obtained and force can be calculated.[80–82] Even early EHTs showed a high degree of longitudinal orientation, intercellular coupling, and force generation,[78,83] and drugs like chromanol, quinidine, erythromycin, and doxorubicin exerted expected responses.[84] Later, using hPSC cardiomyocytes, often in combination with skin fibroblasts,[85] EHTs were also shown to exhibit expected physiological responses to cardioactive stimuli[86] and drugs,[87] outperforming 2D hPSC cardiomyocyte models and isolated rabbit cardiomyocytes in predicting response of inotropic drugs.[22] Moreover, in this particular study, EHTs were the only model—apart from the isolated rabbit cardiomyocytes—that showed a positive force-frequency relationship (FFR). Ventricular hPSC cardiomyocytes have mostly been used to build EHTs, but this has recently been extended to atrial cardiomyocytes. Right atrial hPSC-EHTs had faster contraction kinetics, lower force generation, shorter action potential duration, and higher repolarization fraction than ventricular-like EHTs.[88]

Engineered human myocardium (EHM) is similar to EHT but is generated by integrating the cell-gel mixture with nylon mesh tabs instead of pillars.[89] In addition to static stress and electrical pacing, uniaxial tension can also be exerted. Sarcomeres appeared more aligned under static stress compared with no stress or 1 Hz/4 days of cyclic stress.[89] Cord-like structures, some containing lumens, were observed when ECs were added to the EHMs, and these increased markedly when stromal cells (mouse embryonic fibroblasts or human bone marrow stromal cells) were also added.[89]

More complex EHT designs can include a single implanted platinum wire to induce more physiological activation of a propagation wave in the tissue, rather than whole-field stimulation with 2 electrodes that activate all cells in the tissue simultaneously.[90] EHTs as rings, where tissues compact around a central rod,[91] provide EHTs without anchoring zones, thus isometric contraction (contraction without change in length); of note, although easier to reproduce, isometric contraction is less physiological than auxotonic contractile work on elastomeric pillars.[83]

Both types of engineered tissues have been used for modeling cardiomyopathies, since they are particularly suited to measuring changes in contraction force associated with these conditions. For example, dilated cardiomyopathy,[92–94] hypertrophic cardiomyopathy,[85,95–98] and familial cardiomyopathy[99] have been investigated. The majority of the studies included mutant cardiomyocytes in EHTs, while one study induced hypertrophy by chronic β-adrenergic stimulation.[85] Cell interactions that take place in myocardial interstitial fibrosis were investigated by including excess pericytes; the study showed fibrotic tissue responses marked by decreased contractility, increased tissue stiffness, secretion of BNP, and upregulated myofibroblast-associated genes.[100]

In general, casting cardiac cells in hydrogels results in highly reproducible cardiac tissues with unidirectional force of contraction. EHTs and EHMs thus represent a valuable tradeoff between the fully controlled MTFs and self-assembled scaffold-free cardiac tissues.

Cardiac Wires

CWs were developed to provide both structural cues and electrical field stimulation with view to enhancing hiPSC-cardiomyocyte maturation. CWs also use cell-hydrogel mixes but can be cast in PDMS channels with an anchored surgical suture in line with the channel.[101] An updated version has 2 parallel poly-octamethylene maleate (anhydride) citrate wires fixed at both ends of the microwell.[102] In both versions, the tissue experiences high longitudinal tension, which facilitates uniaxial contraction and alignment. Displacement of the wires enables quantification of passive tension and active force, but Ca^{2+} transients and electrical properties can also be measured.[23,101] Cardiomyocytes in CWs also show canonical responses to compounds that act via β-adrenergic/cAMP pathway (isoproterenol and milrinone), L-type Ca^{2+} channel (FPL64176 and nifedipine), or indirectly affect intracellular Ca^{2+} concentrations (digoxin). Positive inotropic drugs induced expected responses in these tissues.[103] Additionally, CWs have been used to model left ventricular hypertrophy.[102] While most engineered myocardium generated from hPSCs is ventricular like, heteropolar cardiac tissues containing distinct atrial and ventricular ends have also been developed (atrioventricular CW).[102] Perfusion through the wire mimics vascularization of the heart.[104] Fibrosis was also modeled by increasing the CF content and using a fibrin-based hydrogel to encapsulate the cells. This enabled quantification of collagen deposition, which is increased in fibrotic myocardium.[105] These heterogeneous CWs allowed the effects of antifibrotic compounds to be examined on equivalents of the scar lesion, border zone, and adjacent healthy myocardium simultaneously, with convenient functional readouts.[105] A variant I-wire system enabled the culture of 3D cardiac tissues between titanium wires to form an elongated cardiac muscle.[106] Here, an integrated flexible probe provided strain loading via lateral displacement. Passive tension and active contractility can be quantified by optical measurement (fluorescent probe or tissue displacement), and the tissue can be electrically stimulated or subjected to sustained mechanical load.[107]

Downloaded from http://ahajournals.org by on March 22, 2021

Microfluidic Platforms

Organs-on-Chips, where tissues are integrated in engineered microfluidic chips, now include heart-on-chip modalities. Microfluidic channels lined with ECs can mimic blood vessels and the crucial dialogue between cardiomyocytes and ECs undergoing blood flow or interaction with inflammatory cells and cytokines.

Pulsatile tubular cardiac tissues were generated with cell sheets containing hiPSC cardiomyocytes and human dermal fibroblasts and then wrapping these sheets around a flexible octagonal column. Small slits on the sides of the column in these bioreactors allowed pulsation and perfusion (0.5 mL/min). Spontaneous beating or electrical stimulation of the tissues resulted in electrical and inner pressure changes.[108] Mimics of pumping heart chambers were also developed that were uniquely able to measure pressure and volume metrics, and pressure load could be controlled with an adjustable hydrostatic fluid column.[109] In another approach, the gel-cell mix was seeded between multiple microposts to form a 3D tissue flanked by 2 medium channels; an integrated pneumatic actuation system induced homogeneous uniaxial cyclic strain to the tissue.[110] Incorporation of electrodes allowed mechanical and biochemical costimulation of this heart-on-chip.[111] A microfluidic device with 4 compartments was also developed. It consisted of a microchannel, chamber, diaphragm, and a push bar that controlled the volume of the microchannel. Displacement of the beating tissue, measured using fluorescent particles in the microchannel, indicated positive FFR in this device.[112]

SCAFFOLDS AND MATRIX: DO THESE MATTER?

In contrast to conventional (2D) cultures, which are typically on rigid polystyrene (PS), scaffold-based tissues are usually cultured on substrates that have mechanical properties more closely resembling those of the cellular niche, such as silicone rubbers or gels. The most widely used material for this purpose is PDMS, which is easy to manipulate, gas-permeable allowing oxygen diffusion, optically transparent, and biocompatible. However, while PS is far from inert, PDMS is notorious for drug absorption, which was thought to be related to compound hydrophobicity but is more likely related to its topological polar surface area.[113] As an example of how PS and PDMS differ, the concentration of cardioactive drug bepridil after 3 hours in the culture medium was reduced by ≈50% by tissue-culture PS but over ≈80% by PDMS.[113] A particularly useful feature of PDMS in cardiac tissue engineering, however, is its availability in different stiffnesses and elasticities allowing changes in cardiomyocyte (after)load and thus the force generated.[21] In contrast to PS with a fixed Young modulus of ≈3.7 GPa,[114] PDMS stiffness can be tuned within a physiological range,[115] allowing healthy (load, <50 kPa) or diseased (eg, fibrotic; load, ±100 kPa) cardiac environments to be modeled.[116] More instantaneous changes in afterload during culture can be achieved by inserting metal braces in the pillars of EHTs. This has been shown to induce cardiomyocyte enlargement of 28.4% in neonatal rat tissues—a hallmark of pathological hypertrophy.[117] Another approach to tuning pillar stiffness uses magnetic beads.[118] Translational applications, especially those concerning disease modeling, can benefit from use of these more complex, physiologically relevant substrate materials, but difficulty in predicting the extent to which they can reduce compound bioavailability still limits their use in pharmaceutical screening pipelines.

Besides scaffold material, ECM also plays an important role in determining the (patho)physiological nature of the model, since this fibrous protein network provides a biological niche for tissue assembly and its physical features govern cell behavior. ECM is known to closely interact with cells by presenting growth factors to their receptors and sensing and transducing mechanical signals, which influences cell growth, morphology, function, migration, survival, gene expression, and differentiation.[119] In scaffold-free cardiac tissues, ECM is self-secreted, but in scaffold-based tissues, it is mostly added exogenously. Differences in chemical and mechanical properties contribute to cardiomyocyte alignment, intracellular organization, and force in seeded tissues.[23,120,121] While it has not yet been possible to rely on ECM self-secretion to form cardiac EHTs, this might be a way forward ensuring only physiologically relevant ECMs are actually present.

To control and manipulate stiffness in vitro, ECMs can be electrospun to align the fibers or the hydrogel concentration can be changed.[122] There are now even methods that allow ECM or hydrogel stiffness to be modulated during cell culture by temperature or light.[123] There are many ECM types in humans, of which collagen, fibronectin, and elastin are most common in the healthy human heart.[124] These are present in precisely controlled ratios that may be altered in disease states. For example, collagen I:III ratio is ≈0.6 in healthy hearts but ≈1.2 in dilated cardiomyopathic hearts.[125] Careful selection and control of the composition of ECM might, therefore, be important for disease modeling in vitro. Nevertheless, many cardiac tissue engineering approaches do not take this into account and even use ECMs not present in the healthy heart but, like fibrin,[126] for example, only formed during scaring after MI. The composition and mechanical but also thermal properties of the ECM are also extremely important when used for 3D bioprinting as these characteristics determine the resolution achievable in the bioprinted models. Moreover, in some cases, material properties can affect cell viability due to the extrusion process through the nozzle.[127] When engineered cardiac tissues are used for heart regeneration, scaffold and ECM need to be compliant

Downloaded from http://ahajournals.org by on March 22, 2021

with good manufacturing practice. Clinical-grade ECMs are available but are typically expensive although might be replaced by engineered ECM.[128] For cotransplanted scaffold carriers for the cardiac tissues, biodegradable materials also offer solutions.[129]

MATURATION IN 3D CARDIAC MODELS

Immaturity is an important shortcoming of hPSC cardiomyocytes for modeling cardiac disease or drug responses in adults since ordinarily they do not develop further than the equivalent of 16 weeks for human gestation.[130] One motivation for developing 3D cardiac tissues was to increase the maturation state of hPSC cardiomyocytes so that their functional and structural properties are more like native adult tissue. This means increased contraction force, positive FFR, post-rest potentiation (PRP) and Frank-Starling law, greater sarcomere organization and length, electrical coupling through gap junctions, higher mitochondria number and alignment with sarcomeres, mitochondrial cristae development, the presence of transverse tubules, and metabolic switch from glucose to fatty acids. Although in many studies, relative rather than absolute values for these parameters are reported, the overall degree of maturation in any 3D cardiac model is improved compared with standard 2D culture even though none have yet achieved that of adult cardiomyocytes. In some cases, maturation has been promoted not only by the 3D environment but also by reproducing (via external stimulation) the mechanical load and the electrical pacing regime that cardiomyocytes experience in the heart. Mechanical load can result in auxotonic contraction (more physiological, most like that in EHTs[131]) or stretch in the tissue. Afterload also plays an important role in functional maturation of cardiomyocytes in EHTs.[117,132] While moderate afterload promotes cardiomyocyte maturation, further increase may be detrimental and cause pathological changes.[133] Here, we discuss in more detail maturation in structure, function, and metabolism in the different models.

Structure

Many scaffold-based 3D models and some scaffold-free 3-cell type cardiac microtissues achieve sarcomere lengths and organization similar to adult cardiomyocytes.[134,135] In general though, scaffold-free cardiac tissues have been analyzed in less depth than scaffold-based tissues (Table 1).

Microtissues showed increased myofibrillar organization over time when hiPSC-cardiomyocyte purity was <50% at the beginning of 3D culture. This was an early indication that undefined noncardiomyocyte cells present may affect initial aggregation and maturation.[33] Microtissues containing hESC cardiomyocytes, HUVECs (human umbilical vein endothelial cells), and mouse embryonic fibroblasts indeed showed enhanced collagen production and mechanical stiffness.[34] Subsequent studies on 1/2/3-cell type microtissues found structural maturation in scaffold-free microtissues, with enhanced ECM (collagen, fibronectin, and laminin) deposition[30,35,40] and increased expression of the mature isoforms of sarcomeric proteins.[20,31,35,37,38] We also showed enhanced sarcomere organization and length using cardiomyocytes, ECs, and CFs from hiPSCs concurrently in 3-cell type microtissues.[20]

The first (large) rat EHTs[78,79] and later (smaller) hESC cardiomyocyte/fibrin-based EHTs with fewer cells similarly showed enhanced cardiomyocyte alignment and well-developed sarcomere organization. CX43 junctional protein expression was evident although not confined to intercalated discs as in adult heart.[80] Structural maturation was also observed in EHMs, reflected in an increase in the MYL7:MYL2 ratio, cardiomyocyte alignment, and (physiological) hypertrophy.[85] Using hiPSC cardiomyocytes expressing the genetically encoded Ca^{2+} indicator GCaMP3, looped activation propagation was found in EHT rings, together with improved structural maturation and enhanced adult cardiac gene expression in a frequency-dependent manner.[136] After transfer to a silicon stretcher, both ventricular- and atrial-like EHT rings underwent similar structural and functional maturation.[137] In EHMs subjected to passive stress, an optimal stretch distance resulted in aligned cardiomyocytes, mechanical contractions throughout the whole tissue, coordinated Ca^{2+} waves, and upregulation of genes associated with maturation without the need for cyclic stretch.[107]

Long-term electrical stimulation for cardiomyocyte maturation was first reported in nonhuman EHTs.[79,138] Biphasic pacing (1 week at 2 Hz, the next at 1.5 Hz) for 4 days after EHT formation improved sarcomere ultrastructure, with regular M bands, increased CX43 abundance, and improved external Ca^{2+} response. When pacing was increased to supraphysiological levels for 3 weeks, much greater maturation was reported with sarcomere lengths of ≈2.2 μm and strikingly mature features in histology.[126] However, this report has recently been extensively corrected and has yet to be reproduced by others. Interestingly, inflammatory gene expression was detected in stimulated EHTs, likely due to oxidative stress caused by the electrical pacing.[139,140] Also in CWs, increasing pacing improved ultrastructural organization (frequent myofibril convergence with sarcomeres, aligned Z discs, numerous mitochondria, desmosomes, many H zones per sarcomere and I bands per Z disc) and increased cardiomyocyte size.[23,101]

Function

Notably, all models still show spontaneous beating, with depolarized resting membrane potentials compared with adult cardiomyocyte (≈—90 mV) and other immature functional features (Table 2). However, the beat rates in microtissues and EHTs vary between studies, ranging from 20 to 80 bpm (Table 2).

Downloaded from http://ahajournals.org by on March 22, 2021

Electrophysical properties of cardiomyocytes in 3D cardiac tissues are technically difficult to measure but can be analyzed using impaling electrodes or first dissociating the tissue into single cells for conventional patch-clamp analysis. Voltage-sensitive dyes have also been used although they are less sensitive and do not provide absolute measures of all parameters. Different techniques and cellular components in microtissues have led to a wide range of electrophysiology values being reported. For example, voltage-sensitive dyes in cardiomyocyte-only microtissues showed increased action potential duration and upstroke velocity[40] (Table 2), while sharp-electrode patch clamp in microtissues with CFs and hiPSC cardiomyocytes showed rather slow upstroke velocities (66 V/s) and depolarized (more positive) resting membrane potential (—41 mV)[31]; 3-cell type microtissues by contrast showed longer action potential duration, hyperpolarized resting membrane potential, and faster upstroke velocities, independent of whether measured by patch clamp in whole-tissue microtissues or as single cells after dissociation.[20]

Electrophysical properties in EHTs were typical of more mature cardiomyocytes, with similar I_{Na} density and upstroke velocities as in human ventricular tissue.[25,80,126,141] Recently, I_{to} notches were reported in the AP profile of CWs measured with sharp-electrode patch clamp.[102] The positive PRP in hPSC-EHTs, albeit small, indicated the capacity of the sarcoplasmic reticulum to store and release Ca^{2+}.[87]

Contraction kinetics of microtissues and EHTs also differed quantitatively between studies (Table 2). Multicell type composition promotes functional maturation, as cardiomyocytes in 3-cell type microtissues showed enhanced contractile function (higher beating rate and Ca^{2+} transient amplitude) and expected responses to ionotropic drugs, through upregulation of sarcomeric and calcium-binding proteins, compared with cardiomyocyte-only 3D culture.[37]

To assess contractility, conduction velocity (CV) and contraction force are informative parameters, but they can be measured only in some (mostly scaffold based) models. In 3D printed microtissues, CV and contraction force have been assessed using voltage-sensitive dyes. CV was relatively slow (≈2–3 versus 30–100 cm/s in adult human heart),[53] but contraction force increased with time in culture, although could not be measured absolutely since the needle tip was not microscopically uniform.[54] One study measured contraction force in cardiac cell sheets by placing sheets onto fibrin gels in a customized device.[142] This showed contractile force around 1 mN and 3.3 mN/mm^2 of cross-sectional area, higher than in some other models but still far from that of the adult human heart (40–50 mN/mm^2).[143] The study showed positive Frank-Starling relationship but negative FFR, again indicating some but not complete maturation.[142] Cell sheets do allow cell alignment by micropatterning of the cell culture surface[144]; this may also improve cardiomyocyte contractile function.

In EHMs, the force of contraction increased to 6.2±0.8 mN/mm^2 at 1.5 Hz[85] after 8 weeks of culture, which is higher than the force of contraction in papillary muscle from human infants (≈1 mN/mm^2 at 1 Hz)[145] but still lower than in healthy adult myocardium. Interestingly, the force-length relationship was similar to the Frank-Starling curves in intact heart.[85] Nevertheless, it was claimed that these EHMs only resembled the 13-week human fetal heart.[85,89,107]

Electrical stimulation (5 V/cm, 2 Hz, 5 ms) in combination with static stretch causes cell alignment, physiological hypertrophy, increased force (1.34±0.19 mN/mm^2), and Frank-Starling–like force-length relationships. In addition, functional maturation associated with enhanced expression of sarcoplasmic reticulum–related proteins SERCA2 (sarco-endoplasmic reticulum calcium ATPase 2) and RYR2 (ryanodine receptor 2) was observed.[82] Stepwise increases in cyclic stress of EHM cultured between 2 titanium rods resulted in improved sarcomere alignment, cardiomyocyte coupling, and active tension (4.4 mN/mm^2), claimed to be comparable with native myocardium.[146,147] Higher contraction force was reported after biphasic pacing in EHTs; however, it was still lower (≈0.23 mN) than in adult cardiomyocytes, mitochondria were immature, and the sensitivity to Ca^{2+} remained too high.[139] Pacing at supraphysiological levels produced positive FFR,[126] characteristic of human adult ventricular myocardium, but also seen in earlier EHT models.[85] Since positive FFR might be masked by increased funny current (I_f) that triggers spontaneous contraction in hPSC cardiomyocytes, the I_f blocker ivabradine has been used to induce quiescence before measuring FFR, which is then investigated by pacing the tissue at lower frequencies (0.75–2.5 Hz), which revealed a positive FFR.[86]

Several studies indicated that hPSC cardiomyocytes in CWs respond much the same way to pacing as EHTs: gradual increase toward 6 Hz produced more mature CV, electrophysiology, and Ca^{2+} handling.[23,101,126] The authors hypothesized that 6 Hz stimulation (twice that of the human fetal heart) could be a compensatory mechanism for the lack of noncardiomyocytes, indirectly resulting in cardiomyocyte maturation.[101] Addition of increasing numbers of CFs in CWs increased passive tension and decreased active force. Moreover, adding fibrin to the collagen hydrogel improved intracellular organization of cardiomyocytes. These tissues showed adult-like functionality and maturation: positive FFRs, substantial PRPs, and active force measurements up to 16 μN.[23] In blinded validation, drug-induced changes on CWs were examined. Inotropes with different mechanisms of action (including β-adrenergic agonists, PDE3 inhibitors, Ca^{2+} sensitizers, myosin and troponin activators, and an apelin receptor agonist) could be distinguished, adding this to the models that may be predictive for new therapeutics.[148] Interestingly, robust positive FFR, PRP, and fast

Downloaded from http://ahajournals.org by on March 22, 2021

CVs were observed, although these were still below that of adult myocardium (30–100 cm/s).[102]

Microfluidics was also shown to improve functional maturation in heart-on-chip models. Dynamic conditions (platform rocker, 30° tilt, 0.4 Hz) yielded 2.5-fold higher active force compared with static conditions, physiological Frank-Starling mechanism, increased cardiomyocyte density and hypertrophy (Table 2).[149] Biomimetic systems using a pressure gradient to move fluid through the cardiac system as in the native heart showed that physiological mechanical loads and biaxial stretch did not substantially improve cardiomyocyte maturation.[150] In contrast, cyclic stretching (5%), electrical stimulation (1 Hz), and vascular perfusion of 0.2 mL/min did improve maturation.

Metabolism

Metabolic maturation is rarely reported in 3D cardiac models. Two studies using microtissues and different methods to assess metabolism showed energetically more efficient glucose metabolism, with reduced glycolysis and enhanced mitochondrial oxidative phosphorylation.[20,40] Most EHTs have been cultured in glucose-based media, mimicking the metabolic state of fetal hearts.[151] However, culture medium with low carbohydrates, low insulin, no serum, and palmitate changed EHT metabolism toward fatty acids and also induced some degree of maturation.[25] Passive stretch has also been shown to cause a similar metabolic switch in hiPSC cardiomyocytes from EHTs.[152] Key proliferation pathways (β-catenin and Yes-associated protein 1) were repressed, force increased, Ca^{2+} handling was more mature, mitochondrial mass was increased, and overall organization improved[25] (Tables 1 and 2).

HOW 3D CARDIAC TISSUES COULD BE USED IN REGENERATIVE MEDICINE

The human heart is limited in its capacity to regenerate since it appears to lack cardiomyocyte stem cells and adult cardiomyocytes divide only slowly.[153] Repair after damage is then largely through scar tissue formation. Restoration of healthy myocardium to maintain proper contractile function and conductivity is essential to prevent subsequent heart failure or arrhythmogenic behavior, respectively, and various approaches are currently being investigated for this purpose (Figure 2). They include directed transdifferentiation of CFs to cardiomyocytes in situ[154] and replacement of cardiomyocytes by transplantation of hPSC cardiomyocytes.[3] Unless donor derived, hPSC cardiomyocytes would require lifelong immunosuppression to prevent rejection. In addition, both direct reprogramming and ectopic cardiomyocyte transplantation would need careful control of potential arrhythmogenic risk and ways to ensure that sufficient but not excessive cardiomyocyte numbers are present in the heart. First transplantation studies of hPSC cardiomyocyte suspensions into the heart were performed in rodents, later in nonhuman primates.[155–160] Cell delivery was intracoronary, intravenous, or intramyocardial. This was reported to attenuate cardiac remodeling,[161] improve vascularization,[162] and (transiently) improve cardiac function.[156,163,164] Absence of electrical coupling with host tissue[155] was always a limitation, sometimes causing malignant ventricular arrhythmia.[162,165] Poor retention and survival of hPSC cardiomyocytes was often observed,[166,167] although scaffold embedding with pro-survival factors prevented apoptosis after transplantation, resulting in low engraftment efficiency.[161]

An alternative cardiac regeneration and repair that could overcome these limitations is the use of multicell type 3D cardiac (engineered) tissues containing hPSC cardiomyocytes for transplantation (Figure 2). As hPSC cardiomyocyte suspensions, teratomas were not observed after transplantation of (engineered) tissues,[168] and these could be constructed without animal components, paving the way for good manufacturing practice compliance in humans.[82,85,168] Specialized catheters were required for delivery[169,170] and, for larger tissue constructs, open chest surgery.[171,172] In another approach, cell sheets of nonhuman primate ESC-derived SSEA-1^+ cells (described as cardiac progenitors) and adipose tissue–derived stromal cells were transplanted into the hearts of primates where they engrafted and differentiated in situ into cardiomyocytes.[173]

One of the first studies to restore myocardial function in vivo in rat hearts used collagen-based EHTs from neonatal rat cardiomyocytes.[174] Although hPSC-derived cardiomyocytes in EHTs and EHMs survived and engrafted (with up to 25% of the transplanted cells retained until week 12),[168] ultimately there was no functional benefit compared with cell free controls.[168,175,176] Lack of electromechanical coupling or vascularization is often the cause. Electromechanical coupling was seen in microtissue-based size-controlled (through number of input microtissues) patches,[33] which, more generally, can be constructed from different cardiac cell types and used for direct injection or as building blocks to generate tissue engineered constructs.[35] When bioprinted 3D cardiac tissues (2×2 cm×400 μm) composed of human fetal heart $SCA1^+$-derived cells in hyaluronic acid/gelatin-based matrix were transplanted epicardially onto ischemic mouse hearts, engraftment and long-term survival were observed.[177] These printed cardiac patches resulted in smaller scars, improved cardiac function, and better cardiomyocyte survival compared with the control group.[178] Cardiac patches can also be printed using microtissues containing hiPSC cardiomyocytes, ECs, and fibroblasts, without biomaterials, and following transplantation to rat heart, they become vascularized from the host.[53] Enhanced cardiac function was observed in rat hearts after MI first using

Downloaded from http://ahajournals.org by on March 22, 2021

rat cardiomyocyte–derived cell sheets[179] but later using either hiPSC cardiomyocytes alone[180–182] or hiPSC cardiomyocytes with hiPSC vascular cells (ECs and mural cells).[183,184] hiPSC cardiomyocytes were also used in combination with hiPSC ECs in transplantable EHTs, and these improved left ventricular function after implantation in MI guinea pig hearts.[175] The importance of multiple cell types was also seen in microtissues containing cardiomyocytes, CFs, and ECs on a fibrin-based patch, which even showed vascularization after positioning over the infarcted region of the mouse heart, electromechanical coupling, and over 25% engraftment; this resulted in improved cardiac function in vivo in mouse hearts.[185] Multilayered cardiac cell sheets consisting of different cell types to form patches also facilitated microvessel sprouting into the host cardiomyocyte layer and coupling with the host vasculature improving cell survival and maturation.[184,186] More recently, multicell type bioprinted constructs containing hiPSC cardiomyocytes and HUVECs encapsulated in hydrogel strands with alginate and PEG-fibrinogen were shown to improve integration in vivo.[187]

Optimization of the grafts in vitro using similar approaches as described for tissue maturation is promising to improve 3D constructs for translation. Cyclic stretch, electrical stimulation, and vascular network formation[188] in hPSC-derived EHTs before engraftment increased contractile and intercellular organization and may facilitate perfusion by the host coronary circulation,[189] evidenced by host erythrocytes in the constructs.[89] Importantly, hiPSC-derived EHTs were transplanted into guinea pigs after MI, and electrical activity was telemetrically monitored in the heart for 28 days. This showed there was no clinically relevant sustained ventricular tachycardia or ventricular fibrillation, suggesting electrical safety.[190] Of note, this approach allowed the contractile performance of the EHT to be determined before implantation, which may benefit further optimization.[106]

Alternatively, the substrate of the patch can be engineered to facilitate coupling or vascular sprouting. For example, hESC cardiomyocytes were plated on to a prepatterned vascular bed of aligned microchannels,[36] which induced neoangiogenesis and vascular remodeling.[36] These perfusable grafts supported cardiomyocyte survival and integration with the host coronary vessels after transplantation in vivo into infarcted rat hearts much better than nonperfused constructs.[176] Cardiac tissues cultured on these AngioChips and implanted to the femoral vessels of rat hind limbs in which ischemia had been induced underwent immediate blood reperfusion,[191] suggesting that perfusable engineered microvasculature would promote formation of large vascularized 3D cardiac constructs suitable for regenerative therapy. Similarly, printed vascularized cardiac patches of 2- to 7-mm thickness, containing hiPSC cardiomyocytes and hiPSC ECs in hydrogel with blood vessel architecture optimized for oxygen transfer using mathematical modeling, showed elongated cardiomyocytes in vitro with striking actinin striation, high cell viability, and strong contractile activity.[192] Printing small-diameter blood vessels within thick structures is challenging, but multiphoton 3D printing has been used to create native-like scaffolds from ECM, which contained hiPSC cardiomyocytes, ECs, and smooth muscle cells (SMCs) (ratio, 2:1:1). After transplantation to mice post-MI, contraction speed was increased and calcium handling improved.[193]

In summary, preformed 3D engineered multicell type (perfusable) cardiac tissues have the potential to form larger grafts than conventional approaches and may provide excellent opportunities for heart repair once severe damage and tissue loss has occurred. Approaches that exploit the potential of in vitro engineering and conditioning aimed at graft optimization for vascular and functional coupling in vivo are among the most likely candidates for safe and effective cardiac repair. The prospect of being able to remuscularize chronic myocardial scars and thus restore cardiac function in patients is far beyond cell transplantation ambitions and could even be performed in late-stage disease provided the surgery is feasible. Further studies that focus on functional coupling and vascularization in nonhuman primates and larger animals in this context are of high relevance.

Gene Therapy

3D cardiac tissues based on human cells could also be used for testing the potential effectiveness of gene therapy (Figure 2): does a construct work in repairing the defective cell type, and how many cells need to be repaired to restore tissue function? This is most important for genetic conditions with now equivalent in animal models. The use of patient-specific hiPSCs in this context can contribute to the realization of personalized medicine. In addition, dedifferentiating adult cardiomyocytes in vivo to enhance reentry into the cell cycle followed by secondary redifferentiation may also be feasible. A proliferative barrier was reported to be imposed by fatty acid metabolism in EHTs and was rescued by simultaneous activation of β-catenin and YAP1 (yes-associated protein 1) using small molecules or genetic activation of these pathways.[25]

CRISPR-Cas9 gene repair has been used directly in 3D organoids although mostly on single cells before inclusion in the 3D tissue or after dissociation because delivery into 3D structures is still technically challenging.[194] However, there are several recent examples of infection using viral vectors directly in 3D, for example, in retinal spheroids using adeno-associated viral vectors.[194,195] This may eventually be used in heart models.

HOW TO CHOOSE A CARDIAC 3D MODEL

Those new to the field may find it challenging to choose between the multiplicity of models now available for the human heart, all claiming to be true tissue mimics and

Downloaded from http://ahajournals.org by on March 22, 2021

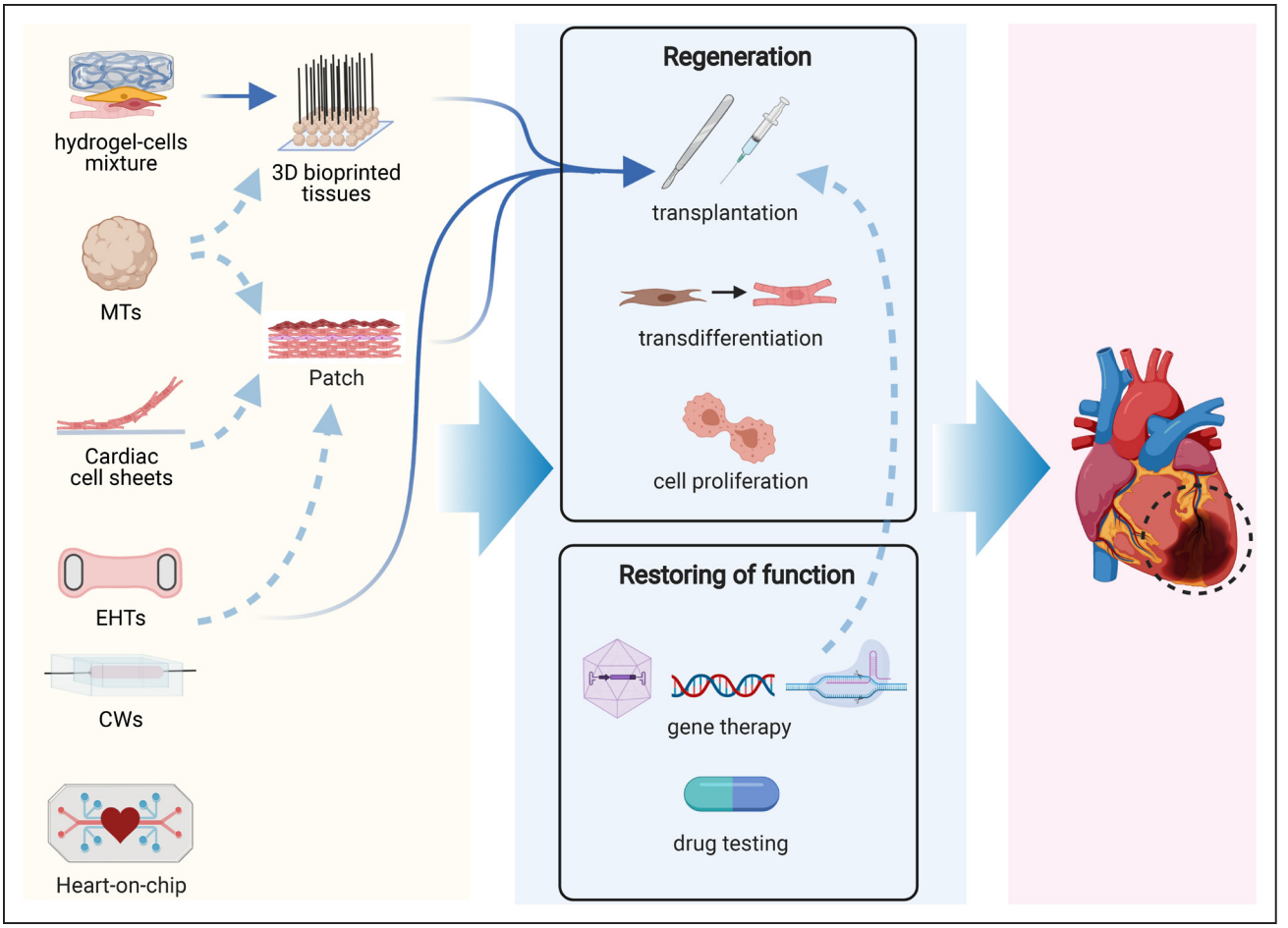

Figure 2. Three-dimensional (3D) cardiac models in regenerative medicine.
Left, Overview of models applicable to cardiac regenerative medicine: microtissues (MTs), cardiac cell sheets, engineered heart tissues (EHTs), and cardiac wires (CWs) can used for transplantation either alone or as cardiac (3D bioprinted) patches. **Middle**, Applications of models in cardiac regenerative medicine, including tissue regeneration and restoration of tissue function. Gene therapy can be also used in addition to or instead of transplantation. **Right**, The ultimate goal is to restore function of damaged hearts in vivo.

to induce tissue maturation to a greater or lesser extent. As we mentioned earlier, a useful guiding principle is to keep a model as simple as possible to address the questions at hand. This means that it is not always necessary to actually rebuild native myocardium. Rather, a balance needs to be found between desired throughput, biological relevance, ease of use, time, cost, and meaningful readouts (Figure 3). This may include consideration of the numbers of cells required, the presence of scaffolds, or the requirement for specialized apparatus, all influencing the throughput. Scaffold-free microtissues self-assemble and meet requirements of simplicity and low cell numbers (2000–5000), reducing costs of each tissue so that their production can be inexpensively scaled. EHTs typically required large cell numbers making them costly, and they could only be produced in small numbers, limiting throughput, for example, in drug screens, or allowing only escalating dose to be measured on a single EHT rather than independent dosing. More recently though, EHTs have undergone miniaturization to 1 µL- or 96-well formats[25,81] using around 15 000 cells. EHTs have the advantage that the scaffold material (hydrogels, synthetic polymers with different viscoelasticities) can easily be modified, and electrical pacing and addition of mechanical load are feasible. The same is true for CWs, which also use few cells but may be more challenging to construct, and in some cases for cardiac patches (fused microtissues or cell sheets).[34,142]

Decisions on which models are most suitable are also dictated by the biological question or application (Figure 3; Table 3). For example, scaffold-free microtissues have significant benefits for (new) drug testing since many tissues can be produced in parallel at low cost and drugs can bind to the scaffolds. Several studies have assessed responses to positive and negative ionotropic drugs[11,20,35,38,39] and cardiotoxins.[30,44,46,196,197] These studies showed that many models can reproduce known drug effects on the heart. Even though throughput is presently lower and costs higher, EHTs have been successfully used for drug testing and are particularly appropriate for long-term measurement of drug responses, since they are more stable than scaffold-free tissues.[198] Both

Downloaded from http://ahajournals.org by on March 22, 2021

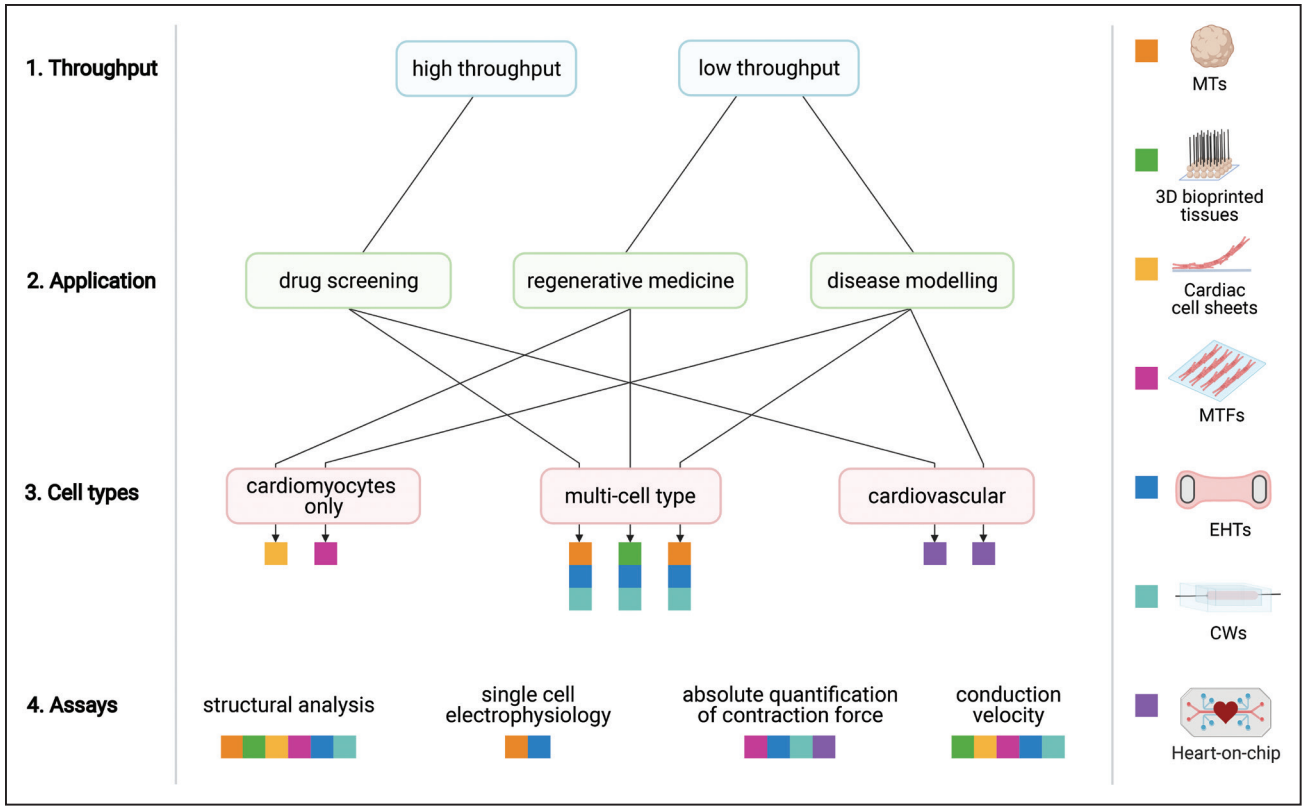

Figure 3. How to choose a 3-dimensional (3D) cardiac model.
Key decision steps (**left**) are numbered in their order. Possible choice paths are indicated by arrows, leading to the different models, each represented by a different color, as indicated (**right**). CW indicates cardiac wire; EHT, engineered heart tissue; MT, microtissue; and MTF, muscle thin film.

Downloaded from http://ahajournals.org by on March 22, 2021

microtissues and EHTs have also been used for disease modeling, as already mentioned, and changing the ratio of different cell types can mimic pathological heart conditions.[105,199,200] Multicell type 3D constructs or microtissues that include both hiPSC cardiomyocytes and noncardiomyocytes[20] are useful for modeling genetic cardiac diseases and investigating whether noncardiomyocyte cells contribute to or cause disease in addition to or instead of cardiomyocytes. This is most appropriate for precision or personalized medicine when all cells are derived from the same genetic background (pairs of genetically corrected and patient cells). Heart-on-chip models incorporate vascular-like fluidic flow through cardiac tissue and are of growing interest to study cardiovascular disease and drugs, where either passage of inflammatory cells or cytokines through the vasculature may affect responses of the heart tissue. However, their added value above simpler models (adding inflammatory cytokines alone) remains to be proven.

Finally, possible assays and readouts need also to be considered in the choice of the model (Figure 3). Absolute values are preferred as they allow comparison between independent studies, relevant to determining the severity of a genetic phenotype or drug responses. Among quantitative parameters that can be obtained for virtually all models are structural organization and contraction based on analysis of video recordings (Tables 1 and 3). Sarcomere organization in cardiomyocytes is fairly straightforward to measure in 2D formats but is more difficult in spheroid tissues like microtissues, where the cardiomyocytes are not precisely oriented. ECM produced in scaffold-free tissues or hydrogels in engineered tissues can make dissociation to single cells difficult and disrupt sarcomeres but when successful allows analysis by single-cell RNA sequencing or patch-clamp electrophysiology. We and others have demonstrated the feasibility of dissociation for microtissues and EHTs.[20,25,126] Scaffold-based tissues allow direct measurement of force of contraction and CV, relevant for modeling conduction defects or cardiomyopathies, while this is not possible in microtissues (Table 2).

OUTLOOK: WHAT FEATURES ARE MISSING IN CURRENT CARDIAC 3D MODELS?

Cardiac 3D models are coming of age in their ability to model healthy human myocardium for testing cardioactive drugs and are poised to contribute more widely to understanding cardiac diseases and even the interaction of the heart with other organs via linked organ-on-chip formats. Clearly, complete maturation and generation of all of the different cardiomyocyte and cardiac stromal cell subtypes found in the adult human heart[201] is still

Table 3. Applications, Readouts, and Advantages of 3D Cardiac Models

	3D cardiac model	Main applications	Readouts	Advantages
Scaffold free	MTs	Drug testing, disease modeling, transplantation	Morphological, contractility, gene expression, Ca^{2+} handling, electrophysiology after dissociation and replating single cells	Small size, low costs, no specialized apparatus, amenable to high-throughput upscaling
	3D printed tissues	Transplantation	Morphological, contractility, gene expression, Ca^{2+} handling, electrophysiology after dissociation and replating single cells	Automated production, highly controlled architecture, biocompatible through autocrine ECM production
	Cell sheets	Transplantation	Morphological, contractility, gene expression, Ca^{2+} handling, electrophysiology after dissociation and replating single cells	Temperature-responsive dissociation, biocompatible through autocrine ECM production, high throughput
Scaffold based	MTFs	Drug testing, disease modeling	Morphological, contractility, gene expression, Ca^{2+} handling, electrophysiology, direct measurements of force	Measure force of contraction on substrate of specific stiffness, possible integration into other systems, high throughput
	EHTs	Drug testing, disease modeling, transplantation	Morphological, contractility, gene expression, Ca^{2+} handling, electrophysiology after dissociation and replating single cells, direct measurements of force	Force of contraction measurement, can be miniaturized and scaled for medium-high throughput
	CWs	Drug testing, disease modeling	Morphological, contractility, gene expression, Ca^{2+} handling, electrophysiology after dissociation and replating single cells, direct measurements of force	Force of contraction measurement, can be miniaturized and scaled for medium-high throughput
	Heart-on-chip	Drug testing, disease modeling	Morphological, contractility, gene expression, Ca^{2+} handling, electrophysiology after dissociation and replating single cells and MEA, direct measurements of force, shear stress, ejection fraction	Controlled vascularization and tissue access via microfluidic flow, potential to integrate various sensors using microfabrication

3D indicates 3 dimensional; CW, cardiac wire; ECM, extracellular matrix; EHT, engineered heart tissue; MEA, multielectrode array; MT, microtissue; and MTF, muscle thin film.

pending, and it is essential to recapitulate the macrostructure of the heart more closely, as often required for modeling diseases.

In addition, knowledge about the interaction between cardiomyocytes and the vascular and lymph systems that may contain immune cells is also progressing. This would not only allow recapitulation of MI resulting, for example, from plaque formation, arterial blockage, or rupture (as in the study by Westein et al[202]), but also the 3 phases of cardiac repair that follow the arterial blockage.[191] This may require development of methods to derive tissue-specific macrophages of the heart[203] and for live imaging of these events through specific (genetic) reporters or sensors. Post-MI remodeling also includes sympathetic hyperinnervation, which can cause arrhythmias; models of this process could be useful in finding alternative treatments to surgical section. Interaction with the liver mediates responses to cardioactive drugs, where some molecules need to be metabolized before becoming functional or, alternatively, are inactivated by the liver before being effective. Linked heart- and liver-on-chip models may provide a solution when fully developed.[204] Finally, the lymph system is important for fluid drainage after infarction, and better understanding of how this works through models that include lymph vasculature may identify new ways of treating cardiac edema. Congenital heart defects are usually caused by abnormal patterning of the heart after cell differentiation has been initiated, and models that could capture linear heart tube formation, looping, and chamber formation and regionalization[205] would be a useful addition to understand how these defects occur. The rapidly developing area of gastruloids may be one to fill this gap: gastruloids derived from mESCs can form relatively advanced stages of gastrulation with anterior-posterior axis formation and left-right asymmetry, which could provide a model for studying ventricular inversion or transposition of the great arteries in situs inversus, should it be possible to achieve similarly advanced stages with hESC or hiPSC.[206–208]

The ability to translate any data derived from cardiac 3D models to the patients is important to demonstrate usability and clinical relevance. Typical measures for assessing cardiac health clinically are ejection fraction output using echocardiogram, electrical activity using ECG, and identification of damage using biomarkers in blood.[209] While the latter are available as in vitro assays, other readouts are very different from those used to assess 3D cardiac models. For example, electrical field potentials measured using multielectrode arrays in vitro have provided estimates of QT prolongation[210] and CV,[211] but this is only a fraction of the information provided by a 12-lead ECG. Engineering 3D multielectrode arrays in combination with mathematical modeling might result in directly translatable readouts of electrical activity. For assessment of contractility, miniaturized ventricular chambers have been developed that can estimate ejection fraction output,[109] but these did not show the physiologically expected increase in ejection fraction with isoproterenol. Another approach might be to use the same image-based quantification technology, such as MUSCLEMOTION,[13] for both in vitro and in vivo

Downloaded from http://ahajournals.org by on March 22, 2021

measurements, but this would require additional mathematical modeling to be able to translate the outcome to clinically meaningful results.

A critical point to develop and validate mathematical models for translational purposes is to compare clinical data with measurements in personalized cardiac 3D models based preferably on patient-specific cells with their isogenic controls. This could eventually demonstrate which model can capture specific complex disease phenotypes and finally contribute to finding novel therapies.

CONCLUSIONS

3D cardiac tissues clearly exhibit many features of native human myocardium, albeit at early postnatal or juvenile stages of development. There are many biophysical conditions that could still be used in combination to advance these models further and increase their utility in disease modeling, revealing the role of novel genetic variants of unknown significance and setting the stage for developing new treatments that are currently unavailable for many chronic conditions of the heart. Providing better and more accessible models is also an important contribution that could be made by academia to the pharmaceutical industry—an incentive to increase efforts not only to treat (rare) genetic conditions but also those resulting from environmental factors, such as lifestyle or side effects of, for example, cancer therapy. Importantly, interaction between environmental and genetic predisposition might be captured using patient hiPSCs.

ARTICLE INFORMATION

Affiliations

Department of Anatomy and Embryology, Leiden University Medical Center, Leiden, the Netherlands (G.C., L.M.W., B.J.v.M., M.B., C.L.M.). MESA+ Institute (B.J.v.M.) and Department of Applied Stem Cell Technologies (C.L.M.), University of Twente, Enschede, the Netherlands. Department of Biology, University of Padua, Italy (M.B.). Veneto Institute of Molecular Medicine, Padua, Padua, Italy (M.B.).

Acknowledgments

Figures were created with BioRender.com.

Sources of Funding

This study was funded by the Netherlands Organ-on-Chip Initiative, an NWO Gravitation project funded by the Ministry of Education, Culture and Science of the government of the Netherlands (024.003.001); European Union Horizon 2020 Research and Innovation Programme under the Marie Sklodowska Curie Actions (individual fellowship, MSCA-IF 838985 SiGNATURE); Transnational Research Project on Cardiovascular Diseases (JTC2016_FP-40-021); and the Netherlands Organisation for Health Research and Development ZonMW (Meer Kennis met Minder Dieren [MKMD]), project No. 114022504).

Disclosures

None.

REFERENCES

1. Takahashi K, Tanabe K, Ohnuki M, Narita M, Ichisaka T, Tomoda K, Yamanaka S. Induction of pluripotent stem cells from adult human fibroblasts by defined factors. *Cell*. 2007;131:861–872. doi: 10.1016/j.cell.2007.11.019
2. Giacomelli E, Mummery CL, Bellin M. Human heart disease: lessons from human pluripotent stem cell-derived cardiomyocytes. *Cell Mol Life Sci*. 2017;74:3711–3739. doi: 10.1007/s00018-017-2546-5
3. Nakamura K, Murry CE. Function follows form - a review of cardiac cell therapy. *Circ J*. 2019;83:2399–2412. doi: 10.1253/circj.CJ-19-0567
4. Zhang M, D'Aniello C, Verkerk AO, Wrobel E, Frank S, Ward-Van Oostwaard D, Piccini I, Freund C, Rao J, Seebohm G, et al. Recessive cardiac phenotypes in induced pluripotent stem cell models of Jervell and Lange-Nielsen syndrome: disease mechanisms and pharmacological rescue. *Proc Natl Acad Sci USA*. 2014;111:E5383–E5392. doi:10.1073/pnas.1419553111.
5. Davis RP, Casini S, van den Berg CW, Hoekstra M, Remme CA, Dambrot C, Salvatori D, Oostwaard DW, Wilde AA, Bezzina CR, et al. Cardiomyocytes derived from pluripotent stem cells recapitulate electrophysiological characteristics of an overlap syndrome of cardiac sodium channel disease. *Circulation*. 2012;125:3079–3091. doi: 10.1161/CIRCULATIONAHA.111.066092
6. Jung CB, Moretti A, Mederos y Schnitzler M, Iop L, Storch U, Bellin M, Dorn T, Ruppenthal S, Pfeiffer S, Goedel A, et al. Dantrolene rescues arrhythmogenic RYR2 defect in a patient-specific stem cell model of catecholaminergic polymorphic ventricular tachycardia. *EMBO Mol Med*. 2012;4:180–191. doi: 10.1002/emmm.201100194
7. Blinova K, Dang Q, Millard D, Smith G, Pierson J, Guo L, Brock M, Lu HR, Kraushaar U, Zeng H, et al. International multisite study of human-induced pluripotent stem cell-derived cardiomyocytes for drug proarrhythmic potential assessment. *Cell Rep*. 2018;24:3582–3592. doi: 10.1016/j.celrep.2018.08.079
8. Harris K, Aylott M, Cui Y, Louttit JB, McMahon NC, Sridhar A. Comparison of electrophysiological data from human-induced pluripotent stem cell-derived cardiomyocytes to functional preclinical safety assays. *Toxicol Sci*. 2013;134:412–426. doi: 10.1093/toxsci/kft113
9. Caspi O, Itzhaki I, Kehat I, Gepstein A, Arbel G, Huber I, Satin J, Gepstein L. In vitro electrophysiological drug testing using human embryonic stem cell derived cardiomyocytes. *Stem Cells Dev*. 2009;18:161–172. doi: 10.1089/scd.2007.0280
10. Braam SR, Tertoolen L, van de Stolpe A, Meyer T, Passier R, Mummery CL. Prediction of drug-induced cardiotoxicity using human embryonic stem cell-derived cardiomyocytes. *Stem Cell Res*. 2010;4:107–116. doi:10.1016/j.scr.2009.11.004.
11. Pointon A, Pilling J, Dorval T, Wang Y, Archer C, Pollard C. From the cover: high-throughput imaging of cardiac microtissues for the assessment of cardiac contraction during drug discovery. *Toxicol Sci*. 2017;155:444–457. doi: 10.1093/toxsci/kfw227
12. Ribeiro MC, Tertoolen LG, Guadix JA, Bellin M, Kosmidis G, D'Aniello C, Monshouwer-Kloots J, Goumans MJ, Wang YL, Feinberg AW, et al. Functional maturation of human pluripotent stem cell derived cardiomyocytes in vitro–correlation between contraction force and electrophysiology. *Biomaterials*. 2015;51:138–150. doi: 10.1016/j.biomaterials.2015.01.067
13. Sala L, van Meer BJ, Tertoolen LGJ, Bakkers J, Bellin M, Davis RP, Denning C, Dieben MAE, Eschenhagen T, Giacomelli E, et al. MUSCLEMOTION: a versatile open software tool to quantify cardiomyocyte and cardiac muscle contraction in vitro and in vivo. *Circ Res*. 2018;122:e5–e16. doi: 10.1161/CIRCRESAHA.117.312067
14. van Meer BJ, Krotenberg A, Sala L, Davis RP, Eschenhagen T, Denning C, Tertoolen LGJ, Mummery CL. Simultaneous measurement of excitation-contraction coupling parameters identifies mechanisms underlying contractile responses of hiPSC-derived cardiomyocytes. *Nat Commun*. 2019;10:4325. doi: 10.1038/s41467-019-12354-8
15. Birket MJ, Ribeiro MC, Kosmidis G, Ward D, Leitoguinho AR, van de Pol V, Dambrot C, Devalla HD, Davis RP, Mastroberardino PG, et al. Contractile defect caused by mutation in MYBPC3 revealed under conditions optimized for human PSC-cardiomyocyte function. *Cell Rep*. 2015;13:733–745. doi: 10.1016/j.celrep.2015.09.025
16. Kim C, Wong J, Wen J, Wang S, Wang C, Spiering S, Kan NG, Forcales S, Puri PL, Leone TC, et al. Studying arrhythmogenic right ventricular dysplasia with patient-specific iPSCs. *Nature*. 2013;494:105–110. doi: 10.1038/nature11799
17. Dorn T, Kornherr J, Parrotta EI, Zawada D, Ayetey H, Santamaria G, Iop L, Mastantuono E, Sinnecker D, Goedel A, et al. Interplay of cell–cell contacts and RhoA/ MRTF -a signaling regulates cardiomyocyte identity. *EMBO J*. 2018;37:e98133. doi: 10.15252/embj.201798133
18. Martewicz S, Luni C, Serena E, Pavan P, Chen HV, Rampazzo A, Elvassore N. Transcriptomic characterization of a human in vitro model of arrhythmogenic

Downloaded from http://ahajournals.org by on March 22, 2021

cardiomyopathy under topological and mechanical stimuli. *Ann Biomed Eng*. 2019;47:852–865. doi: 10.1007/s10439-018-02134-8
19. Bliley JM, Vermeer M, Duffy RM, Batalov I, Kramer D, Tashman JW, Shiwarski DJ, Lee A, Teplenin A, Volkers L, et al. Dynamic loading of human engineered heart tissue enhances contractile function and drives desmosome-linked disease phenotype. *BioRxiv*. Preprint posted online June 04, 2020. doi:10.1101/2020.05.25.111690.
20. Giacomelli E, Meraviglia V, Campostrini G, Cochrane A, Cao X, van Helden RWJ, Krotenberg Garcia A, Mircea M, Kostidis S, Davis RP, et al. Human-iPSC-derived cardiac stromal cells enhance maturation in 3D cardiac microtissues and reveal non-cardiomyocyte contributions to heart disease. *Cell Stem Cell*. 2020;26:862–879.e11. doi: 10.1016/j.stem.2020.05.004
21. Hersch N, Wolters B, Dreissen G, Springer R, Kirchgeßner N, Merkel R, Hoffmann B. The constant beat: cardiomyocytes adapt their forces by equal contraction upon environmental stiffening. *Biol Open*. 2013;2:351–361. doi: 10.1242/bio.20133830
22. Saleem U, van Meer BJ, Katili PA, Mohd Yusof NAN, Mannhardt I, Garcia AK, Tertoolen L, de Korte T, Vlaming MLH, McGlynn K, et al. Blinded, multicenter evaluation of drug-induced changes in contractility using human-induced pluripotent stem cell-derived cardiomyocytes. *Toxicol Sci*. 2020;176:103–123. doi: 10.1093/toxsci/kfaa058
23. Zhao Y, Rafatian N, Wang EY, Feric NT, Lai BFL, Knee-Walden EJ, Backx PH, Radisic M. Engineering microenvironment for human cardiac tissue assembly in heart-on-a-chip platform. *Matrix Biol*. 2020;85–86:189–204. doi: 10.1016/j.matbio.2019.04.001
24. Ribeiro AJ, Ang YS, Fu JD, Rivas RN, Mohamed TM, Higgs GC, Srivastava D, Pruitt BL. Contractility of single cardiomyocytes differentiated from pluripotent stem cells depends on physiological shape and substrate stiffness. *Proc Natl Acad Sci USA*. 2015;112:12705–12710. doi: 10.1073/pnas.1508073112
25. Mills RJ, Titmarsh DM, Koenig X, Parker BL, Ryall JG, Quaife-Ryan GA, Voges HK, Hodson MP, Ferguson C, Drowley L, et al. Functional screening in human cardiac organoids reveals a metabolic mechanism for cardiomyocyte cell cycle arrest. *Proc Natl Acad Sci USA*. 2017;114:E8372–E8381. doi: 10.1073/pnas.1707316114
26. Huebsch N, Loskill P, Deveshwar N, Spencer CI, Judge LM, Mandegar MA, Fox CB, Mohamed TM, Ma Z, Mathur A, et al. Miniaturized iPS-cell-derived cardiac muscles for physiologically relevant drug response analyses. *Sci Rep*. 2016;6:24726. doi: 10.1038/srep24726
27. Mummery C, Ward-van Oostwaard D, Doevendans P, Spijker R, van den Brink S, Hassink R, van der Heyden M, Opthof T, Pera M, de la Riviere AB, et al. Differentiation of human embryonic stem cells to cardiomyocytes: role of coculture with visceral endoderm-like cells. *Circulation*. 2003;107:2733–2740. doi: 10.1161/01.CIR.0000068356.38592.68
28. Tan Y, Richards D, Coyle RC, Yao J, Xu R, Gou W, Wang H, Menick DR, Tian B, Mei Y. Cell number per spheroid and electrical conductivity of nanowires influence the function of silicon nanowired human cardiac spheroids. *Acta Biomater*. 2017;51:495–504. doi: 10.1016/j.actbio.2017.01.029
29. Brown DA, MacLellan WR, Laks H, Dunn JC, Wu BM, Beygui RE. Analysis of oxygen transport in a diffusion-limited model of engineered heart tissue. *Biotechnol Bioeng*. 2007;97:962–975. doi: 10.1002/bit.21295
30. Polonchuk L, Chabria M, Badi L, Hoflack JC, Figtree G, Davies MJ, Gentile C. Cardiac spheroids as promising in vitro models to study the human heart microenvironment. *Sci Rep*. 2017;7:7005. doi: 10.1038/s41598-017-06385-8
31. Beauchamp P, Jackson CB, Ozhathil LC, Agarkova I, Galindo CL, Sawyer DB, Suter TM, Zuppinger C. 3D co-culture of hiPSC-derived cardiomyocytes with cardiac fibroblasts improves tissue-like features of cardiac spheroids. *Front Mol Biosci*. 2020;7:14. doi: 10.3389/fmolb.2020.00014
32. Yang B, Lui C, Yeung E, Matsushita H, Jeyaram A, Pitaktong I, Inoue T, Mohamed Z, Ong CS, DiSilvestre D, et al. A net mold-based method of biomaterial-free three-dimensional cardiac tissue creation. *Tissue Eng Part C Methods*. 2019;25:243–252. doi: 10.1089/ten.TEC.2019.0003
33. Stevens KR, Pabon L, Muskheli V, Murry CE. Scaffold-free human cardiac tissue patch created from embryonic stem cells. *Tissue Eng Part A*. 2009;15:1211–1222. doi: 10.1089/ten.tea.2008.0151
34. Stevens KR, Kreutziger KL, Dupras SK, Korte FS, Regnier M, Muskheli V, Nourse MB, Bendixen K, Reinecke H, Murry CE. Physiological function and transplantation of scaffold-free and vascularized human cardiac muscle tissue. *Proc Natl Acad Sci USA*. 2009;106:16568–16573. doi: 10.1073/pnas.0908381106
35. Richards DJ, Coyle RC, Tan Y, Jia J, Wong K, Toomer K, Menick DR, Mei Y. Inspiration from heart development: biomimetic development of functional human cardiac organoids. *Biomaterials*. 2017;142:112–123. doi: 10.1016/j.biomaterials.2017.07.021
36. Noguchi R, Nakayama K, Itoh M, Kamohara K, Furukawa K, Oyama JI, Node K, Morita S. Development of a three-dimensional pre-vascularized scaffold-free contractile cardiac patch for treating heart disease. *J Heart Lung Transplant*. 2016;35:137–145. doi: 10.1016/j.healun.2015.06.001
37. Ravenscroft SM, Pointon A, Williams AW, Cross MJ, Sidaway JE. Cardiac non-myocyte cells show enhanced pharmacological function suggestive of contractile maturity in stem cell derived cardiomyocyte microtissues. *Toxicol Sci*. 2016;152:99–112. doi: 10.1093/toxsci/kfw069
38. Giacomelli E, Bellin M, Sala L, van Meer BJ, Tertoolen LG, Orlova VV, Mummery CL. Three-dimensional cardiac microtissues composed of cardiomyocytes and endothelial cells co-differentiated from human pluripotent stem cells. *Development*. 2017;144:1008–1017. doi: 10.1242/dev.143438
39. Devarasetty M, Forsythe S, Shupe TD, Soker S, Bishop CE, Atala A, Skardal A. Optical tracking and digital quantification of beating behavior in bioengineered human cardiac organoids. *Biosensors*. 2017;7:24. doi: 10.3390/bios7030024
40. Correia C, Koshkin A, Duarte P, Hu D, Carido M, Sebastião MJ, Gomes-Alves P, Elliott DA, Domian IJ, Teixeira AP, et al. 3D aggregate culture improves metabolic maturation of human pluripotent stem cell derived cardiomyocytes. *Biotechnol Bioeng*. 2018;115:630–644. doi: 10.1002/bit.26504
41. Halbert SP, Bruderer R, Lin TM. In vitro organization of dissociated rat cardiac cells into beating three-dimensional structures. *J Exp Med*. 1971;133:677–695. doi: 10.1084/jem.133.4.677
42. Kelm JM, Ehler E, Nielsen LK, Schlatter S, Perriard JC, Fussenegger M. Design of artificial myocardial microtissues. *Tissue Eng*. 2004;10:201–214. doi: 10.1089/107632704322791853
43. Garzoni LR, Rossi MI, de Barros AP, Guarani V, Keramidas M, Balottin LB, Adesse D, Takiya CM, Manso PP, Otazú IB, et al. Dissecting coronary angiogenesis: 3D co-culture of cardiomyocytes with endothelial or mesenchymal cells. *Exp Cell Res*. 2009;315:3406–3418. doi: 10.1016/j.yexcr.2009.09.016
44. Archer CR, Sargeant R, Basak J, Pilling J, Barnes JR, Pointon A. Characterization and validation of a human 3D cardiac microtissue for the assessment of changes in cardiac pathology. *Sci Rep*. 2018;8:10160. doi: 10.1038/s41598-018-28393-y
45. Sebastião MJ, Gomes-Alves P, Reis I, Sanchez B, Palacios I, Serra M, Alves PM. Bioreactor-based 3D human myocardial ischemia/reperfusion in vitro model: a novel tool to unveil key paracrine factors upon acute myocardial infarction. *Transl Res*. 2020;215:57–74. doi: 10.1016/j.trsl.2019.09.001
46. Richards DJ, Li Y, Kerr CM, Yao J, Beeson GC, Coyle RC, Chen X, Jia J, Damon B, Wilson R, et al. Human cardiac organoids for the modelling of myocardial infarction and drug cardiotoxicity. *Nat Biomed Eng*. 2020;4:446–462. doi: 10.1038/s41551-020-0539-4
47. Roche CD, Brereton RJL, Ashton AW, Jackson C, Gentile C. Current challenges in three-dimensional bioprinting heart tissues for cardiac surgery. *Eur J Cardiothorac Surg*. 2020;58:500–510. doi: 10.1093/ejcts/ezaa093
48. Puluca N, Lee S, Doppler S, Münsterer A, Dreßen M, Krane M, Wu SM. Bioprinting approaches to engineering vascularized 3D cardiac tissues. *Curr Cardiol Rep*. 2019;21:90. doi: 10.1007/s11886-019-1179-8
49. Romanazzo S, Nemec S, Roohani I. iPSC bioprinting: where are we at? *Materials (Basel)*. 2019;12:2453. doi: 10.3390/ma12152453
50. Fonseca AC, Melchels FPW, Ferreira MJS, Moxon SR, Potjewyd G, Dargaville TR, Kimber SJ, Domingos M. Emulating human tissues and organs: a bioprinting perspective toward personalized medicine. *Chem Rev*. 2020;120:11128–11174. doi: 10.1021/acs.chemrev.0c00342
51. Alonzo M, AnilKumar S, Roman B, Tasnim N, Joddar B. 3D bioprinting of cardiac tissue and cardiac stem cell therapy. *Transl Res*. 2019;211:64–83. doi: 10.1016/j.trsl.2019.04.004
52. Moldovan NI. Progress in scaffold-free bioprinting for cardiovascular medicine. *J Cell Mol Med*. 2018;22:2964–2969. doi: 10.1111/jcmm.13598
53. Ong CS, Fukunishi T, Zhang H, Huang CY, Nashed A, Blazeski A, DiSilvestre D, Vricella L, Conte J, Tung L, et al. Biomaterial-free three-dimensional bioprinting of cardiac tissue using human induced pluripotent stem cell derived cardiomyocytes. *Sci Rep*. 2017;7:4566. doi:10.1038/s41598-017-05018-4
54. Arai K, Murata D, Verissimo AR, Mukae Y, Itoh M, Nakamura A, Morita S, Nakayama K. Fabrication of scaffold-free tubular cardiac constructs using a bio-3D printer. *PLoS One*. 2018;13:e0209162. doi: 10.1371/journal.pone.0209162
55. Arai K, Murata D, Takao S, Nakamura A, Itoh M, Kitsuka T, Nakayama K. Drug response analysis for scaffold-free cardiac constructs fabricated using bio-3D printer. *Sci Rep*. 2020;10:8972. doi: 10.1038/s41598-020-65681-y

Downloaded from http://ahajournals.org by on March 22, 2021

56. LaBarge W, Morales A, Pretorius D, Kahn-Krell AM, Kannappan R, Zhang J. Scaffold-free bioprinter utilizing layer-by-layer printing of cellular spheroids. *Micromachines*. 2019;10:570. doi: 10.3390/mi10090570
57. Haraguchi Y, Shimizu T, Yamato M, Okano T. Regenerative therapies using cell sheet-based tissue engineering for cardiac disease. *Cardiol Res Pract*. 2011;2011:845170. doi: 10.4061/2011/845170
58. Kim K, Bou-Ghannam S, Okano T. Cell sheet tissue engineering for scaffold-free three-dimensional (3D) tissue reconstruction. *Methods Cell Biol*. 2020;157:143–167. doi: 10.1016/bs.mcb.2019.11.020
59. Okano T, Yamada N, Sakai H, Sakurai Y. A novel recovery system for cultured cells using plasma-treated polystyrene dishes grafted with poly(N-isopropylacrylamide). *J Biomed Mater Res*. 1993;27:1243–1251. doi: 10.1002/jbm.820271005
60. Yang J, Yamato M, Shimizu T, Sekine H, Ohashi K, Kanzaki M, Ohki T, Nishida K, Okano T. Reconstruction of functional tissues with cell sheet engineering. *Biomaterials*. 2007;28:5033–5043. doi: 10.1016/j.biomaterials.2007.07.052
61. Haraguchi Y, Shimizu T, Yamato M, Kikuchi A, Okano T. Electrical coupling of cardiomyocyte sheets occurs rapidly via functional gap junction formation. *Biomaterials*. 2006;27:4765–4774. doi: 10.1016/j.biomaterials.2006.04.034
62. Sekiya S, Shimizu T, Yamato M, Kikuchi A, Okano T. Bioengineered cardiac cell sheet grafts have intrinsic angiogenic potential. *Biochem Biophys Res Commun*. 2006;341:573–582. doi: 10.1016/j.bbrc.2005.12.217
63. Shimizu T, Yamato M, Isoi Y, Akutsu T, Setomaru T, Abe K, Kikuchi A, Umezu M, Okano T. Fabrication of pulsatile cardiac tissue grafts using a novel 3-dimensional cell sheet manipulation technique and temperature-responsive cell culture surfaces. *Circ Res*. 2002;90:e40. doi: 10.1161/hh0302.105722
64. Grosberg A, Alford PW, McCain ML, Parker KK. Ensembles of engineered cardiac tissues for physiological and pharmacological study: heart on a chip. *Lab Chip*. 2011;11:4165–4173. doi: 10.1039/c1lc20557a
65. Salick MR, Napiwocki BN, Sha J, Knight GT, Chindhy SA, Kamp TJ, Ashton RS, Crone WC. Micropattern width dependent sarcomere development in human ESC-derived cardiomyocytes. *Biomaterials*. 2014;35:4454–4464. doi: 10.1016/j.biomaterials.2014.02.001
66. Feinberg AW, Feigel A, Shevkoplyas SS, Sheehy S, Whitesides GM, Parker KK. Muscular thin films for building actuators and powering devices. *Science*. 2007;317:1366–1370. doi: 10.1126/science.1146885
67. Alford PW, Feinberg AW, Sheehy SP, Parker KK. Biohybrid thin films for measuring contractility in engineered cardiovascular muscle. *Biomaterials*. 2010;31:3613–3621. doi: 10.1016/j.biomaterials.2010.01.079
68. Shim J, Grosberg A, Nawroth JC, Kit Parker K, Bertoldi K. Modeling of cardiac muscle thin films: pre-stretch, passive and active behavior. *J Biomech*. 2012;45:832–841. doi:10.1016/j.jbiomech.2011.11.024
69. Gaio N, van Meer B, Solano WQ, Bergers L, van de Stolpe A, Mummery C, Sarro PM, Dekker R. Cytostretch, an organ-on-chip platform. *Micromachines*. 2016;7:120. doi: 10.3390/mi7070120
70. Agarwal A, Goss JA, Cho A, McCain ML, Parker KK. Microfluidic heart on a chip for higher throughput pharmacological studies. *Lab Chip*. 2013;13:3599–3608. doi: 10.1039/c3lc50350j
71. Feinberg AW, Alford PW, Jin H, Ripplinger CM, Werdich AA, Sheehy SP, Grosberg A, Parker KK. Controlling the contractile strength of engineered cardiac muscle by hierarchal tissue architecture. *Biomaterials*. 2012;33:5732–5741. doi: 10.1016/j.biomaterials.2012.04.043
72. McCain ML, Agarwal A, Nesmith HW, Nesmith AP, Parker KK. Micromolded gelatin hydrogels for extended culture of engineered cardiac tissues. *Biomaterials*. 2014;35:5462–5471. doi: 10.1016/j.biomaterials.2014.03.052
73. Kuo PL, Lee H, Bray MA, Geisse NA, Huang YT, Adams WJ, Sheehy SP, Parker KK. Myocyte shape regulates lateral registry of sarcomeres and contractility. *Am J Pathol*. 2012;181:2030–2037. doi: 10.1016/j.ajpath.2012.08.045
74. Wang G, McCain ML, Yang L, He A, Silvio Pasqualini F, Agarwal A, Yuan H, Jiang D, Zhang D, Zangi L, et al. Modeling the mitochondrial cardiomyopathy of Barth syndrome with induced pluripotent stem cell and heart-on-chip technologies. *Nat Med*. 2014;20:616–623. doi: 10.1038/nm.3545
75. Park SJ, Zhang D, Qi Y, Li Y, Lee KY, Bezzerides VJ, Yang P, Xia S, Kim SL, Liu X, et al. Insights into the pathogenesis of catecholaminergic polymorphic ventricular tachycardia from engineered human heart tissue. *Circulation*. 2019;140:390–404. doi: 10.1161/CIRCULATIONAHA.119.039711
76. Lind JU, Yadid M, Perkins I, O'Connor BB, Eweje F, Chantre CO, Hemphill MA, Yuan H, Campbell PH, Vlassak JJ, et al. Cardiac microphysiological devices with flexible thin-film sensors for higher-throughput drug screening. *Lab Chip*. 2017;17:3692–3703. doi: 10.1039/c7lc00740j
77. Grosberg A, Nesmith AP, Goss JA, Brigham MD, McCain ML, Parker KK. Muscle on a chip: in vitro contractility assays for smooth and striated muscle. *J Pharmacol Toxicol Methods*. 2012;65:126–135. doi: 10.1016/j.vascn.2012.04.001
78. Eschenhagen T, Fink C, Remmers U, Scholz H, Wattchow J, Weil J, Zimmermann W, Dohmen HH, Schäfer H, Bishopric N, et al. Three-dimensional reconstitution of embryonic cardiomyocytes in a collagen matrix: a new heart muscle model system. *FASEB J*. 1997;11:683–694. doi: 10.1096/fasebj.11.8.9240969
79. Zimmermann WH, Fink C, Kralisch D, Remmers U, Weil J, Eschenhagen T. Three-dimensional engineered heart tissue from neonatal rat cardiac myocytes. *Biotechnol Bioeng*. 2000;68:106–114.
80. Schaaf S, Shibamiya A, Mewe M, Eder A, Stöhr A, Hirt MN, Rau T, Zimmermann WH, Conradi L, Eschenhagen T, et al. Human engineered heart tissue as a versatile tool in basic research and preclinical toxicology. *PLoS One*. 2011;6:e26397. doi: 10.1371/journal.pone.0026397
81. Dostanić M, Windt LM, Stein JM, Van Meer BJ, Bellin M, Orlova V, Mastrangeli M, Mummery C, Sarro PM. A miniaturized EHT platform for accurate measurements of tissue contractile properties. *J Microelectromechanical Syst*. 2020;29:881–887. doi:10.1109/JMEMS.2020.3011196.
82. Ruan JL, Tulloch NL, Razumova MV, Saiget M, Muskheli V, Pabon L, Reinecke H, Regnier M, Murry CE. Mechanical stress conditioning and electrical stimulation promote contractility and force maturation of induced pluripotent stem cell-derived human cardiac tissue. *Circulation*. 2016;134:1557–1567. doi: 10.1161/CIRCULATIONAHA.114.014998
83. Zimmermann WH, Schneiderbanger K, Schubert P, Didié M, Münzel F, Heubach JF, Kostin S, Neuhuber WL, Eschenhagen T. Tissue engineering of a differentiated cardiac muscle construct. *Circ Res*. 2002;90:223–230. doi: 10.1161/hh0202.103644
84. Hansen A, Eder A, Bönstrup M, Flato M, Mewe M, Schaaf S, Aksehirlioglu B, Schwoerer AP, Schwörer A, Uebeler J, et al. Development of a drug screening platform based on engineered heart tissue. *Circ Res*. 2010;107:35–44. doi: 10.1161/CIRCRESAHA.109.211458
85. Tiburcy M, Hudson JE, Balfanz P, Schlick S, Meyer T, Chang Liao ML, Levent E, Raad F, Zeidler S, Wingender E, et al. Defined engineered human myocardium with advanced maturation for applications in heart failure modeling and repair. *Circulation*. 2017;135:1832–1847. doi: 10.1161/CIRCULATIONAHA.116.024145
86. Saleem U, Mannhardt I, Braren I, Denning C, Eschenhagen T, Hansen A. Force and calcium transients analysis in human engineered heart tissues reveals positive force-frequency relation at physiological frequency. *Stem Cell Reports*. 2020;14:312–324. doi: 10.1016/j.stemcr.2019.12.011
87. Mannhardt I, Breckwoldt K, Letuffe-Brenière D, Schaaf S, Schulz H, Neuber C, Benzin A, Werner T, Eder A, Schulze T, et al. Human engineered heart tissue: analysis of contractile force. *Stem Cell Reports*. 2016;7:29–42. doi: 10.1016/j.stemcr.2016.04.011
88. Lemme M, Ulmer BM, Lemoine MD, Zech ATL, Flenner F, Ravens U, Reichenspurner H, Rol-Garcia M, Smith G, Hansen A, et al. Atrial-like engineered heart tissue: an in vitro model of the human atrium. *Stem Cell Reports*. 2018;11:1378–1390. doi: 10.1016/j.stemcr.2018.10.008
89. Tulloch NL, Muskheli V, Razumova MV, Korte FS, Regnier M, Hauch KD, Pabon L, Reinecke H, Murry CE. Growth of engineered human myocardium with mechanical loading and vascular coculture. *Circ Res*. 2011;109:47–59. doi: 10.1161/CIRCRESAHA.110.237206
90. Thavandiran N, Dubois N, Mikryukov A, Massé S, Beca B, Simmons CA, Deshpande VS, McGarry JP, Chen CS, Nanthakumar K, et al. Design and formulation of functional pluripotent stem cell-derived cardiac microtissues. *Proc Natl Acad Sci USA*. 2013;110:E4698–E4707. doi: 10.1073/pnas.1311120110
91. Eschenhagen T, Didié M, Heubach J, Ravens U, Zimmermann WH. Cardiac tissue engineering. *Transpl Immunol*. 2002;9:315–321. doi: 10.1016/s0966-3274(02)00011-4
92. Hinson JT, Chopra A, Nafissi N, Polacheck WJ, Benson CC, Swist S, Gorham J, Yang L, Schafer S, Sheng CC, et al. HEART DISEASE. Titin mutations in iPS cells define sarcomere insufficiency as a cause of dilated cardiomyopathy. *Science*. 2015;349:982–986. doi: 10.1126/science.aaa5458
93. Stillitano F, Turnbull IC, Karakikes I, Nonnenmacher M, Backeris P, Hulot JS, Kranias EG, Hajjar RJ, Costa KD. Genomic correction of familial cardiomyopathy in human engineered cardiac tissues. *Eur Heart J*. 2016;37:3282–3284. doi: 10.1093/eurheartj/ehw307
94. Streckfuss-Bömeke K, Tiburcy M, Fomin A, Luo X, Li W, Fischer C, Özcelik C, Perrot A, Sossalla S, Haas J, et al. Severe DCM phenotype of patient harboring RBM20 mutation S635A can be modeled by patient-specific induced pluripotent stem cell-derived cardiomyocytes. *J Mol Cell Cardiol*. 2017;113:9–21. doi: 10.1016/j.yjmcc.2017.09.008
95. Hinson JT, Chopra A, Lowe A, Sheng CC, Gupta RM, Kuppusamy R, O'Sullivan J, Rowe G, Wakimoto H, Gorham J, et al. Integrative analysis of PRKAG2 cardiomyopathy iPS and microtissue models identifies AMPK as a regulator of metabolism, survival, and fibrosis. *Cell Rep*. 2016;17:3292–3304. doi: 10.1016/j.celrep.2016.11.066

Downloaded from http://ahajournals.org by on March 22, 2021

96. Cashman TJ, Josowitz R, Johnson BV, Gelb BD, Costa KD. Human engineered cardiac tissues created using induced pluripotent stem cells reveal functional characteristics of BRAF-mediated hypertrophic cardiomyopathy. *PLoS One*. 2016;11:e0146697. doi: 10.1371/journal.pone.0146697
97. Ma Z, Huebsch N, Koo S, Mandegar MA, Siemons B, Boggess S, Conklin BR, Grigoropoulos CP, Healy KE. Contractile deficits in engineered cardiac microtissues as a result of MYBPC3 deficiency and mechanical overload. *Nat Biomed Eng*. 2018;2:955–967. doi: 10.1038/s41551-018-0280-4
98. Prondzynski M, Lemoine MD, Zech AT, Horváth A, Di Mauro V, Koivumäki JT, Kresin N, Busch J, Krause T, Krämer E, et al. Disease modeling of a mutation in α-actinin 2 guides clinical therapy in hypertrophic cardiomyopathy. *EMBO Mol Med*. 2019;11:e11115. doi: 10.15252/emmm.201911115
99. Yang KC, Breitbart A, De Lange WJ, Hofsteen P, Futakuchi-Tsuchida A, Xu J, Schopf C, Razumova MV, Jiao A, Boucek R, et al. Novel adult-onset systolic cardiomyopathy due to MYH7 E848G mutation in patient-derived induced pluripotent stem cells. *JACC Basic Transl Sci*. 2018;3:728–740. doi: 10.1016/j.jacbts.2018.08.008
100. Szepes M, Melchert A, Dahlmann J, Hegermann J, Werlein C, Jonigk D, Haverich A, Martin U, Olmer R, Gruh I. Dual function of iPSC-derived pericyte-like cells in vascularization and fibrosis-related cardiac tissue remodeling in vitro. *Int J Mol Sci*. 2020;21:8947. doi: 10.3390/ijms21238947
101. Nunes SS, Miklas JW, Liu J, Aschar-Sobbi R, Xiao Y, Zhang B, Jiang J, Massé S, Gagliardi M, Hsieh A, et al. Biowire: a platform for maturation of human pluripotent stem cell-derived cardiomyocytes. *Nat Methods*. 2013;10:781–787. doi: 10.1038/nmeth.2524
102. Zhao Y, Rafatian N, Feric NT, Cox BJ, Aschar-Sobbi R, Wang EY, Aggarwal P, Zhang B, Conant G, Ronaldson-Bouchard K, et al. A platform for generation of chamber-specific cardiac tissues and disease modeling. *Cell*. 2019;176:913–927.e18. doi: 10.1016/j.cell.2018.11.042
103. Feric NT, Pallotta I, Singh R, Bogdanowicz DR, Gustilo MM, Chaudhary KW, Willette RN, Chendrimada T, Xu X, Graziano MP, et al. Engineered cardiac tissues generated in the biowire II: a platform for human-based drug discovery. *Toxicol Sci*. 2019;172:89–97. doi: 10.1093/toxsci/kfz168
104. Xiao Y, Zhang B, Liu H, Miklas JW, Gagliardi M, Pahnke A, Thavandiran N, Sun Y, Simmons C, Keller G, et al. Microfabricated perfusable cardiac biowire: a platform that mimics native cardiac bundle. *Lab Chip*. 2014;14:869–882. doi: 10.1039/c3lc51123e
105. Wang EY, Rafatian N, Zhao Y, Lee A, Lai BFL, Lu RX, Jekic D, Davenport Huyer L, Knee-Walden EJ, Bhattacharya S, et al. Biowire model of interstitial and focal cardiac fibrosis. *ACS Cent Sci*. 2019;5:1146–1158. doi: 10.1021/acscentsci.9b00052
106. Schroer AK, Shotwell MS, Sidorov VY, Wikswo JP, Merryman WD. I-wire heart-on-a-chip II: biomechanical analysis of contractile, three-dimensional cardiomyocyte tissue constructs. *Acta Biomater*. 2017;48:79–87. doi: 10.1016/j.actbio.2016.11.010
107. Abilez OJ, Tzatzalos E, Yang H, Zhao MT, Jung G, Zöllner AM, Tiburcy M, Riegler J, Matsa E, Shukla P, et al. Passive stretch induces structural and functional maturation of engineered heart muscle as predicted by computational modeling. *Stem Cells*. 2018;36:265–277. doi: 10.1002/stem.2732
108. Tsuruyama S, Matsuura K, Sakaguchi K, Shimizu T. Pulsatile tubular cardiac tissues fabricated by wrapping human iPS cells-derived cardiomyocyte sheets. *Regen Ther*. 2019;11:297–305. doi: 10.1016/j.reth.2019.09.001
109. Li RA, Keung W, Cashman TJ, Backeris PC, Johnson BV, Bardot ES, Wong AOT, Chan PKW, Chan CWY, Costa KD. Bioengineering an electromechanically functional miniature ventricular heart chamber from human pluripotent stem cells. *Biomaterials*. 2018;163:116–127. doi: 10.1016/j.biomaterials.2018.02.024
110. Marsano A, Conficconi C, Lemme M, Occhetta P, Gaudiello E, Votta E, Cerino G, Redaelli A, Rasponi M. Beating heart on a chip: a novel microfluidic platform to generate functional 3D cardiac microtissues. *Lab Chip*. 2016;16:599–610. doi: 10.1039/c5lc01356a
111. Visone R, Talò G, Occhetta P, Cruz-Moreira D, Lopa S, Pappalardo OA, Redaelli A, Moretti M, Rasponi M. A microscale biomimetic platform for generation and electro-mechanical stimulation of 3D cardiac microtissues. *APL Bioeng*. 2018;2:046102. doi: 10.1063/1.5037968
112. Abulaiti M, Yalikun Y, Murata K, Sato A, Sami MM, Sasaki Y, Fujiwara Y, Minatoya K, Shiba Y, Tanaka Y, et al. Establishment of a heart-on-a-chip microdevice based on human iPS cells for the evaluation of human heart tissue function. *Sci Rep*. 2020;10:19201. doi: 10.1038/s41598-020-76062-w
113. van Meer BJ, de Vries H, Firth KSA, van Weerd J, Tertoolen LGJ, Karperien HBJ, Jonkheijm P, Denning C, IJzerman AP, Mummery CL. Small molecule absorption by PDMS in the context of drug response bioassays. *Biochem Biophys Res Commun*. 2017;482:323–328. doi: 10.1016/j.bbrc.2016.11.062
114. Oral I, Guzel H, Ahmetli G. Measuring the Young's modulus of polystyrene-based composites by tensile test and pulse-echo method. *Polym Bull*. 2011;67:1893–1906. doi: 10.1007/s00289-011-0530-z
115. Masterton S, Ahearne M. Influence of polydimethylsiloxane substrate stiffness on corneal epithelial cells. *R Soc Open Sci*. 2019;6:191796. doi: 10.1098/rsos.191796
116. Chaturvedi RR, Herron T, Simmons R, Shore D, Kumar P, Sethia B, Chua F, Vassiliadis E, Kentish JC. Passive stiffness of myocardium from congenital heart disease and implications for diastole. *Circulation*. 2010;121:979–988. doi: 10.1161/CIRCULATIONAHA.109.850677
117. Hirt MN, Sörensen NA, Bartholdt LM, Boeddinghaus J, Schaaf S, Eder A, Vollert I, Stöhr A, Schulze T, Witten A, et al. Increased afterload induces pathological cardiac hypertrophy: a new in vitro model. *Basic Res Cardiol*. 2012;107:307. doi: 10.1007/s00395-012-0307-z
118. Zhao R, Boudou T, Wang WG, Chen CS, Reich DH. Decoupling cell and matrix mechanics in engineered microtissues using magnetically actuated microcantilevers. *Adv Mater*. 2013;25:1699–1705. doi: 10.1002/adma.201203585
119. Rozario T, Desimone DW. The extracellular matrix in development and morphogenesis: a dynamic view. *Dev Biol*. 2009;341:126–140. doi: 10.1016/j.ydbio.2009.10.026
120. Goldfracht I, Efraim Y, Shinnawi R, Kovalev E, Huber I, Gepstein A, Arbel G, Shaheen N, Tiburcy M, Zimmermann WH, et al. Engineered heart tissue models from hiPSC-derived cardiomyocytes and cardiac ECM for disease modeling and drug testing applications. *Acta Biomater*. 2019;92:145–159. doi: 10.1016/j.actbio.2019.05.016
121. Jacot JG, McCulloch AD, Omens JH. Substrate stiffness affects the functional maturation of neonatal rat ventricular myocytes. *Biophys J*. 2008;95:3479–3487. doi: 10.1529/biophysj.107.124545
122. Wang X, Ding B, Li B. Biomimetic electrospun nanofibrous structures for tissue engineering. *Mater Today (Kidlington)*. 2013;16:229–241. doi: 10.1016/j.mattod.2013.06.005
123. Stowers RS, Allen SC, Suggs LJ. Dynamic phototuning of 3D hydrogel stiffness. *Proc Natl Acad Sci USA*. 2015;112:1953–1958. doi: 10.1073/pnas.1421897112
124. Johnson TD, Hill RC, Dzieciatkowska M, Nigam V, Behfar A, Christman KL, Hansen KC. Quantification of decellularized human myocardial matrix: a comparison of six patients. *Proteomics Clin Appl*. 2016;10:75–83. doi: 10.1002/prca.201500048
125. Chen QZ, Harding SE, Ali NN, Lyon AR, Boccaccini AR. Biomaterials in cardiac tissue engineering: ten years of research survey. *Mater Sci Eng R Rep*. 2008;59:1–37. doi: 10.1016/j.mser.2007.08.001
126. Ronaldson-Bouchard K, Ma SP, Yeager K, Chen T, Song L, Sirabella D, Morikawa K, Teles D, Yazawa M, Vunjak-Novakovic G. Advanced maturation of human cardiac tissue grown from pluripotent stem cells. *Nature*. 2018;556:239–243. doi: 10.1038/s41586-018-0016-3
127. Jungst T, Smolan W, Schacht K, Scheibel T, Groll J. Strategies and molecular design criteria for 3D printable hydrogels. *Chem Rev*. 2016;116:1496–1539. doi: 10.1021/acs.chemrev.5b00303
128. Curvello R, Kerr G, Micati DJ, Chan WH, Raghuwanshi VS, Rosenbluh J, Abud HE, Garnier G. Engineered plant-based nanocellulose hydrogel for small intestinal organoid growth. *Adv Sci*. 2021;8:2002135. doi: 10.1002/advs.202002135
129. Sireesha M, Jagadeesh Babu V, Ramakrishna S. Biocompatible and biodegradable elastomer/fibrinogen composite electrospun scaffolds for cardiac tissue regeneration. *RSC Adv*. 2015;5:103308–103314. doi:10.1039/c5ra20322h.
130. van den Berg CW, Okawa S, Chuva de Sousa Lopes SM, van Iperen L, Passier R, Braam SR, Tertoolen LG, del Sol A, Davis RP, Mummery CL. Transcriptome of human foetal heart compared with cardiomyocytes from pluripotent stem cells. *Development*. 2015;142:3231–3238. doi: 10.1242/dev.123810
131. Mills RJ, Hudson JE. Bioengineering adult human heart tissue: how close are we? *APL Bioeng*. 2019;3:010901. doi: 10.1063/1.5070106
132. Truitt R, Mu A, Corbin EA, Vite A, Brandimarto J, Ky B, Margulies KB. Increased afterload augments sunitinib-induced cardiotoxicity in an engineered cardiac microtissue model. *JACC Basic Transl Sci*. 2018;3:265–276. doi: 10.1016/j.jacbts.2017.12.007
133. Leonard A, Bertero A, Powers JD, Beussman KM, Bhandari S, Regnier M, Murry CE, Sniadecki NJ. Afterload promotes maturation of human induced pluripotent stem cell derived cardiomyocytes in engineered heart tissues. *J Mol Cell Cardiol*. 2018;118:147–158. doi: 10.1016/j.yjmcc.2018.03.016
134. Guo Y, Pu WT. Cardiomyocyte maturation: new phase in development. *Circ Res* 2020:1086–1106. doi:10.1161/CIRCRESAHA.119.315862.

Downloaded from http://ahajournals.org by on March 22, 2021

135. Karbassi E, Fenix A, Marchiano S, Muraoka N, Nakamura K, Yang X, Murry CE. Cardiomyocyte maturation: advances in knowledge and implications for regenerative medicine. *Nat Rev Cardiol*. 2020;17:341–359. doi: 10.1038/s41569-019-0331-x
136. Li J, Zhang L, Yu L, Minami I, Miyagawa S, Hörning M, Dong J, Qiao J, Qu X, Hua Y, et al. Circulating re-entrant waves promote maturation of hiPSC-derived cardiomyocytes in self-organized tissue ring. *Commun Biol*. 2020;3:1–12. doi:10.1038/s42003-020-0853-0.
137. Goldfracht I, Protze S, Shiti A, Setter N, Gruber A, Shaheen N, Nartiss Y, Keller G, Gepstein L. Generating ring-shaped engineered heart tissues from ventricular and atrial human pluripotent stem cell-derived cardiomyocytes. *Nat Commun*. 2020;11:75. doi: 10.1038/s41467-019-13868-x
138. Radisic M, Park H, Shing H, Consi T, Schoen FJ, Langer R, Freed LE, Vunjak-Novakovic G. Functional assembly of engineered myocardium by electrical stimulation of cardiac myocytes cultured on scaffolds. *Proc Natl Acad Sci USA*. 2004;101:18129–18134. doi: 10.1073/pnas.0407817101
139. Hirt MN, Boeddinghaus J, Mitchell A, Schaaf S, Börnchen C, Müller C, et al. Functional improvement and maturation of rat and human engineered heart tissue by chronic electrical stimulation. *J Mol Cell Cardiol*. 2014;74:151–161. doi: 10.1016/j.yjmcc.2014.05.009
140. Hikoso S, Yamaguchi O, Nakano Y, Takeda T, Omiya S, Mizote I, Taneike M, Oka T, Tamai T, Oyabu J, et al. The I{kappa}B kinase {beta}/nuclear factor {kappa}B signaling pathway protects the heart from hemodynamic stress mediated by the regulation of manganese superoxide dismutase expression. *Circ Res*. 2009;105:70–79. doi: 10.1161/CIRCRESAHA.108.193318
141. Lemoine MD, Mannhardt I, Breckwoldt K, Prondzynski M, Flenner F, Ulmer B, Hirt MN, Neuber C, Horváth A, Kloth B, et al. Human iPSC-derived cardiomyocytes cultured in 3D engineered heart tissue show physiological upstroke velocity and sodium current density. *Sci Rep*. 2017;7:5464. doi: 10.1038/s41598-017-05600-w
142. Sasaki D, Matsuura K, Seta H, Haraguchi Y, Okano T, Shimizu T. Contractile force measurement of human induced pluripotent stem cell-derived cardiac cell sheet-tissue. *PLoS One*. 2018;13:e0198026. doi: 10.1371/journal.pone.0198026
143. van der Velden J, Klein LJ, van der Bijl M, Huybregts MA, Stooker W, Witkop J, Eijsman L, Visser CA, Visser FC, Stienen GJ. Force production in mechanically isolated cardiac myocytes from human ventricular muscle tissue. *Cardiovasc Res*. 1998;38:414–423. doi: 10.1016/s0008-6363(98)00019-4
144. Takahashi H, Okano T. Thermally-triggered fabrication of cell sheets for tissue engineering and regenerative medicine. *Adv Drug Deliv Rev*. 2019;138:276–292. doi: 10.1016/j.addr.2019.01.004
145. Wiegerinck RF, Cojoc A, Zeidenweber CM, Ding G, Shen M, Joyner RW, Fernandez JD, Kanter KR, Kirshbom PM, Kogon BE, et al. Force frequency relationship of the human ventricle increases during early postnatal development. *Pediatr Res*. 2009;65:414–419. doi: 10.1203/PDR.0b013e318199093c
146. Kensah G, Gruh I, Viering J, Schumann H, Dahlmann J, Meyer H, Skvorc D, Bär A, Akhyari P, Heisterkamp A, et al. A novel miniaturized multimodal bioreactor for continuous in situ assessment of bioartificial cardiac tissue during stimulation and maturation. *Tissue Eng Part C Methods*. 2011;17:463–473. doi: 10.1089/ten.TEC.2010.0405
147. Kensah G, Roa Lara A, Dahlmann J, Zweigerdt R, Schwanke K, Hegermann J, Skvorc D, Gawol A, Azizian A, Wagner S, et al. Murine and human pluripotent stem cell-derived cardiac bodies form contractile myocardial tissue in vitro. *Eur Heart J*. 2013;34:1134–1146. doi: 10.1093/eurheartj/ehs349
148. Qu Y, Feric N, Pallotta I, Singh R, Sobbi R, Vargas HM. Inotropic assessment in engineered 3D cardiac tissues using human induced pluripotent stem cell-derived cardiomyocytes in the Biowire TM II platform. *J Pharmacol Toxicol Methods*. 2020;105:106886. doi: 10.1016/j.vascn.2020.106886
149. Jackman CP, Carlson AL, Bursac N. Dynamic culture yields engineered myocardium with near-adult functional output. *Biomaterials*. 2016;111:66–79. doi: 10.1016/j.biomaterials.2016.09.024
150. Rogers AJ, Fast VG, Sethu P. Biomimetic cardiac tissue model enables the adaption of human induced pluripotent stem cell cardiomyocytes to physiological hemodynamic loads. *Anal Chem*. 2016;88:9862–9868. doi: 10.1021/acs.analchem.6b03105
151. Girard J, Ferré P, Pégorier JP, Duée PH. Adaptations of glucose and fatty acid metabolism during perinatal period and suckling-weaning transition. *Physiol Rev*. 1992;72:507–562. doi: 10.1152/physrev.1992.72.2.507
152. Ulmer BM, Stoehr A, Schulze ML, Patel S, Gucek M, Mannhardt I, Funcke S, Murphy E, Eschenhagen T, Hansen A. Contractile work contributes to maturation of energy metabolism in hiPSC-derived cardiomyocytes. *Stem Cell Reports*. 2018;10:834–847. doi: 10.1016/j.stemcr.2018.01.039
153. Kretzschmar K, Post Y, Bannier-Hélaouët M, Mattiotti A, Drost J, Basak O, Li VSW, van den Born M, Gunst QD, Versteeg D, et al. Profiling proliferative cells and their progeny in damaged murine hearts. *Proc Natl Acad Sci USA*. 2018;115:E12245–E12254. doi: 10.1073/pnas.1805829115
154. Stone NR, Gifford CA, Thomas R, Pratt KJB, Samse-Knapp K, Mohamed TMA, Radzinsky EM, Schricker A, Ye L, Yu P, et al. Context-specific transcription factor functions regulate epigenomic and transcriptional dynamics during cardiac reprogramming. *Cell Stem Cell*. 2019;25:87–102.e9. doi: 10.1016/j.stem.2019.06.012
155. Caspi O, Huber I, Kehat I, Habib M, Arbel G, Gepstein A, Yankelson L, Aronson D, Beyar R, Gepstein L. Transplantation of human embryonic stem cell-derived cardiomyocytes improves myocardial performance in infarcted rat hearts. *J Am Coll Cardiol*. 2007;50:1884–1893. doi: 10.1016/j.jacc.2007.07.054
156. van Laake LW, Passier R, Doevendans PA, Mummery CL. Human embryonic stem cell-derived cardiomyocytes and cardiac repair in rodents. *Circ Res*. 2008;102:1008–1010. doi: 10.1161/CIRCRESAHA.108.175505
157. Kehat I, Khimovich L, Caspi O, Gepstein A, Shofti R, Arbel G, Huber I, Satin J, Itskovitz-Eldor J, Gepstein L. Electromechanical integration of cardiomyocytes derived from human embryonic stem cells. *Nat Biotechnol*. 2004;22:1282–1289. doi: 10.1038/nbt1014
158. Ye L, Chang YH, Xiong Q, Zhang P, Zhang L, Somasundaram P, Lepley M, Swingen C, Su L, Wendel JS, et al. Cardiac repair in a porcine model of acute myocardial infarction with human induced pluripotent stem cell-derived cardiovascular cells. *Cell Stem Cell*. 2014;15:750–761. doi: 10.1016/j.stem.2014.11.009
159. Gepstein L, Ding C, Rahmutula D, Rehemedula D, Wilson EE, Yankelson L, Caspi O, Gepstein A, Huber I, Olgin JE. In vivo assessment of the electrophysiological integration and arrhythmogenic risk of myocardial cell transplantation strategies. *Stem Cells*. 2010;28:2151–2161. doi: 10.1002/stem.545
160. Xue T, Cho HC, Akar FG, Tsang SY, Jones SP, Marbán E, Tomaselli GF, Li RA. Functional integration of electrically active cardiac derivatives from genetically engineered human embryonic stem cells with quiescent recipient ventricular cardiomyocytes: insights into the development of cell-based pacemakers. *Circulation*. 2005;111:11–20. doi: 10.1161/01.CIR.0000151313.18547.A2
161. Laflamme MA, Chen KY, Naumova AV, Muskheli V, Fugate JA, Dupras SK, Reinecke H, Xu C, Hassanipour M, Police S, et al. Cardiomyocytes derived from human embryonic stem cells in pro-survival factors enhance function of infarcted rat hearts. *Nat Biotechnol*. 2007;25:1015–1024. doi: 10.1038/nbt1327
162. Chong JJ, Yang X, Don CW, Minami E, Liu YW, Weyers JJ, Mahoney WM, Van Biber B, Cook SM, Palpant NJ, et al. Human embryonic-stem-cell-derived cardiomyocytes regenerate non-human primate hearts. *Nature*. 2014;510:273–277. doi: 10.1038/nature13233
163. Shiba Y, Filice D, Fernandes S, Minami E, Dupras SK, Biber BV, Trinh P, Hirota Y, Gold JD, Viswanathan M, et al. Electrical integration of human embryonic stem cell-derived cardiomyocytes in a guinea pig chronic infarct model. *J Cardiovasc Pharmacol Ther*. 2014;19:368–381. doi: 10.1177/1074248413520344
164. Fernandes S, Naumova AV, Zhu WZ, Laflamme MA, Gold J, Murry CE. Human embryonic stem cell-derived cardiomyocytes engraft but do not alter cardiac remodeling after chronic infarction in rats. *J Mol Cell Cardiol*. 2010;49:941–949. doi: 10.1016/j.yjmcc.2010.09.008
165. Shiba Y, Gomibuchi T, Seto T, Wada Y, Ichimura H, Tanaka Y, Ogasawara T, Okada K, Shiba N, Sakamoto K, et al. Allogeneic transplantation of iPS cell-derived cardiomyocytes regenerates primate hearts. *Nature*. 2016;538:388–391. doi: 10.1038/nature19815
166. Dow J, Simkhovich BZ, Kedes L, Kloner RA. Washout of transplanted cells from the heart: a potential new hurdle for cell transplantation therapy. *Cardiovasc Res*. 2005;67:301–307. doi: 10.1016/j.cardiores.2005.04.011
167. Zhang M, Methot D, Poppa V, Fujio Y, Walsh K, Murry CE. Cardiomyocyte grafting for cardiac repair: graft cell death and anti-death strategies. *J Mol Cell Cardiol*. 2001;33:907–921. doi: 10.1006/jmcc.2001.1367
168. Riegler J, Tiburcy M, Ebert A, Tzatzalos E, Raaz U, Abilez OJ, Shen Q, Kooreman NG, Neofytou E, Chen VC, et al. Human engineered heart muscles engraft and survive long term in a rodent myocardial infarction model. *Circ Res*. 2015;117:720–730. doi: 10.1161/CIRCRESAHA.115.306985
169. Tabei R, Kawaguchi S, Kanazawa H, Tohyama S, Hirano A, Handa N, Hishikawa S, Teratani T, Kunita S, Fukuda J, et al. Development of a transplant injection device for optimal distribution and retention of human induced pluripotent stem cell–derived cardiomyocytes. *J Heart Lung Transplant*. 2019;38:203–214. doi: 10.1016/j.healun.2018.11.002

Downloaded from http://ahajournals.org by on March 22, 2021

170. Johnson TD, Christman KL. Injectable hydrogel therapies and their delivery strategies for treating myocardial infarction. *Expert Opin Drug Deliv*. 2013;10:59–72. doi: 10.1517/17425247.2013.739156
171. Mihic A, Li J, Miyagi Y, Gagliardi M, Li SH, Zu J, Weisel RD, Keller G, Li RK. The effect of cyclic stretch on maturation and 3D tissue formation of human embryonic stem cell-derived cardiomyocytes. *Biomaterials*. 2014;35:2798–2808. doi: 10.1016/j.biomaterials.2013.12.052
172. Castro L, Geertz B, Reinsch M, Aksehirlioglu B, Hansen A, Eschenhagen T, Reichenspurner H, Weinberger F, Pecha S, et al. Implantation of hiPSC-derived cardiac-muscle patches after myocardial injury in a guinea pig model. *J Vis Exp*. 2019:e58810. doi: 10.3791/58810
173. Bel A, Planat-Bernard V, Saito A, Bonnevie L, Bellamy V, Sabbah L, Bellabas L, Brinon B, Vanneaux V, Pradeau P, et al. Composite cell sheets: a further step toward safe and effective myocardial regeneration by cardiac progenitors derived from embryonic stem cells. *Circulation*. 2010;122:S118–S123. doi: 10.1161/CIRCULATIONAHA.109.927293
174. Eschenhagen T, Didié M, Münzel F, Schubert P, Schneiderbanger K, Zimmermann WH. 3D engineered heart tissue for replacement therapy. *Basic Res Cardiol*. 2002;97(suppl 1):I146–I152. doi: 10.1007/s003950200043.
175. Weinberger F, Breckwoldt K, Pecha S, Kelly A, Geertz B, Starbatty J, Yorgan T, Cheng KH, Lessmann K, Stolen T, et al. Cardiac repair in guinea pigs with human engineered heart tissue from induced pluripotent stem cells. *Sci Transl Med*. 2016;8:363ra148. doi: 10.1126/scitranslmed.aaf8781
176. Redd MA, Zeinstra N, Qin W, Wei W, Martinson A, Wang Y, Wang RK, Murry CE, Zheng Y. Patterned human microvascular grafts enable rapid vascularization and increase perfusion in infarcted rat hearts. *Nat Commun*. 2019;10:584. doi: 10.1038/s41467-019-08388-7
177. Gaetani R, Feyen DA, Verhage V, Slaats R, Messina E, Christman KL, Giacomello A, Doevendans PA, Sluijter JP. Epicardial application of cardiac progenitor cells in a 3D-printed gelatin/hyaluronic acid patch preserves cardiac function after myocardial infarction. *Biomaterials*. 2015;61:339–348. doi: 10.1016/j.biomaterials.2015.05.005
178. Yeung E, Fukunishi T, Bai Y, Bedja D, Pitaktong I, Mattson G, Jeyaram A, Lui C, Ong CS, Inoue T, et al. Cardiac regeneration using human-induced pluripotent stem cell-derived biomaterial-free 3D-bioprinted cardiac patch in vivo. *J Tissue Eng Regen Med*. 2019;13:2031–2039. doi: 10.1002/term.2954
179. Sekine H, Shimizu T, Hobo K, Sekiya S, Yang J, Yamato M, Kurosawa H, Kobayashi E, Okano T. Endothelial cell coculture within tissue-engineered cardiomyocyte sheets enhances neovascularization and improves cardiac function of ischemic hearts. *Circulation*. 2008;118:S145–S152. doi: 10.1161/CIRCULATIONAHA.107.757286
180. Kawamura M, Miyagawa S, Miki K, Saito A, Fukushima S, Higuchi T, Kawamura T, Kuratani T, Daimon T, Shimizu T, et al. Feasibility, safety, and therapeutic efficacy of human induced pluripotent stem cell-derived cardiomyocyte sheets in a porcine ischemic cardiomyopathy model. *Circulation*. 2012;126:S29–S37. doi: 10.1161/CIRCULATIONAHA.111.084343
181. Kawamura M, Miyagawa S, Fukushima S, Saito A, Miki K, Ito E, Sougawa N, Kawamura T, Daimon T, Shimizu T, et al. Enhanced survival of transplanted human induced pluripotent stem cell-derived cardiomyocytes by the combination of cell sheets with the pedicled omental flap technique in a porcine heart. *Circulation*. 2013;128(11 suppl 1):S87–S94. doi: 10.1161/CIRCULATIONAHA.112.000366
182. Kawamura M, Miyagawa S, Fukushima S, Saito A, Miki K, Funakoshi S, Yoshida Y, Yamanaka S, Shimizu T, Okano T, et al. Enhanced therapeutic effects of human iPS cell derived-cardiomyocyte by combined cell-sheets with omental flap technique in porcine ischemic cardiomyopathy model. *Sci Rep*. 2017;7:8824. doi: 10.1038/s41598-017-08869-z
183. Masumoto H, Ikuno T, Takeda M, Fukushima H, Marui A, Katayama S, Shimizu T, Ikeda T, Okano T, Sakata R, et al. Human iPS cell-engineered cardiac tissue sheets with cardiomyocytes and vascular cells for cardiac regeneration. *Sci Rep*. 2014;4:6716. doi: 10.1038/srep06716
184. Ishigami M, Masumoto H, Ikuno T, Aoki T, Kawatou M, Minakata K, Ikeda T, Sakata R, Yamashita JK, Minatoya K. Human iPS cell-derived cardiac tissue sheets for functional restoration of infarcted porcine hearts. *PLoS One*. 2018;13:e0201650. doi: 10.1371/journal.pone.0201650
185. Mattapally S, Zhu W, Fast VG, Gao L, Worley C, Kannappan R, Borovjagin AV, Zhang J. Spheroids of cardiomyocytes derived from human-induced pluripotent stem cells improve recovery from myocardial injury in mice. *Am J Physiol Heart Circ Physiol*. 2018;315:H327–H339. doi: 10.1152/ajpheart.00688.2017
186. Schaefer JA, Guzman PA, Riemenschneider SB, Kamp TJ, Tranquillo RT. A cardiac patch from aligned microvessel and cardiomyocyte patches. *J Tissue Eng Regen Med*. 2018;12:546–556. doi: 10.1002/term.2568
187. Maiullari F, Costantini M, Milan M, Pace V, Chirivì M, Maiullari S, Rainer A, Baci D, Marei HE, Seliktar D, et al. A multi-cellular 3D bioprinting approach for vascularized heart tissue engineering based on HUVECs and iPSC-derived cardiomyocytes. *Sci Rep*. 2018;8:13532. doi: 10.1038/s41598-018-31848-x
188. Lux M, Andrée B, Horvath T, Nosko A, Manikowski D, Hilfiker-Kleiner D, Haverich A, Hilfiker A. In vitro maturation of large-scale cardiac patches based on a perfusable starter matrix by cyclic mechanical stimulation. *Acta Biomater*. 2016;30:177–187. doi: 10.1016/j.actbio.2015.11.006
189. Bargehr J, Ong LP, Colzani M, Davaapil H, Hofsteen P, Bhandari S, Gambardella L, Le Novère N, Iyer D, Sampaziotis F, et al. Epicardial cells derived from human embryonic stem cells augment cardiomyocyte-driven heart regeneration. *Nat Biotechnol*. 2019;37:895–906. doi: 10.1038/s41587-019-0197-9
190. Pecha S, Yorgan K, Röhl M, Geertz B, Hansen A, Weinberger F, Sehner S, Ehmke H, Reichenspurner H, Eschenhagen T, et al. Human iPS cell-derived engineered heart tissue does not affect ventricular arrhythmias in a guinea pig cryo-injury model. *Sci Rep*. 2019;9:9831. doi: 10.1038/s41598-019-46409-z
191. Zhang YS, Arneri A, Bersini S, Shin SR, Zhu K, Goli-Malekabadi Z, Aleman J, Colosi C, Busignani F, Dell'Erba V, et al. Bioprinting 3D microfibrous scaffolds for engineering endothelialized myocardium and heart-on-a-chip. *Biomaterials*. 2016;110:45–59. doi: 10.1016/j.biomaterials.2016.09.003
192. Noor N, Shapira A, Edri R, Gal I, Wertheim L, Dvir T. 3D printing of personalized thick and perfusable cardiac patches and hearts. *Adv Sci (Weinh)*. 2019;6:1900344. doi: 10.1002/advs.201900344
193. Gao L, Kupfer ME, Jung JP, Yang L, Zhang P, Da Sie Y, Tran Q, Ajeti V, Freeman BT, Fast VG, et al. Myocardial tissue engineering with cells derived from human-induced pluripotent stem cells and a native-like, high-resolution, 3-dimensionally printed scaffold. *Circ Res*. 2017;120:1318–1325. doi: 10.1161/CIRCRESAHA.116.310277
194. Gopal S, Rodrigues AL, Dordick JS. Exploiting CRISPR Cas9 in three-dimensional stem cell cultures to model disease. *Front Bioeng Biotechnol*. 2020;8:692. doi: 10.3389/fbioe.2020.00692
195. Garita-Hernandez M, Routet F, Guibbal L, Khabou H, Toualbi L, Riancho L, Reichman S, Duebel J, Sahel J-A, Goureau O, et al. AAV-mediated gene delivery to 3D retinal organoids derived from human induced pluripotent stem cells. *Int J Mol Sci*. 2020;21:994. doi: 10.3390/ijms21030994
196. Forsythe SD, Devarasetty M, Shupe T, Bishop C, Atala A, Soker S, Skardal A. Environmental toxin screening using human-derived 3D bioengineered liver and cardiac organoids. *Front Public Health*. 2018;6:103. doi: 10.3389/fpubh.2018.00103
197. Qiao X, van der Zanden SY, Wander DPA, Borràs DM, Song JY, Li X, van Duikeren S, van Gils N, Rutten A, van Herwaarden T, et al. Uncoupling DNA damage from chromatin damage to detoxify doxorubicin. *Proc Natl Acad Sci USA*. 2020;117:15182–15192. doi: 10.1073/pnas.1922072117
198. Eder A, Vollert I, Hansen A, Eschenhagen T. Human engineered heart tissue as a model system for drug testing. *Adv Drug Deliv Rev*. 2016;96:214–224. doi: 10.1016/j.addr.2015.05.010
199. Lee MO, Jung KB, Jo SJ, Hyun SA, Moon KS, Seo JW, Kim SH, Son MY. Modelling cardiac fibrosis using three-dimensional cardiac microtissues derived from human embryonic stem cells. *J Biol Eng*. 2019;13:15. doi: 10.1186/s13036-019-0139-6
200. van Spreeuwel ACC, Bax NAM, van Nierop BJ, Aartsma-Rus A, Goumans MTH, Bouten CVC. Mimicking cardiac fibrosis in a dish: fibroblast density rather than collagen density weakens cardiomyocyte function. *J Cardiovasc Transl Res*. 2017;10:116–127. doi: 10.1007/s12265-017-9737-1
201. Litviňuková M, Talavera-López C, Maatz H, Reichart D, Worth CL, Lindberg EL, Kanda M, Polanski K, Heinig M, Lee M, et al. Cells of the adult human heart. *Nature*. 2020;588:466–472. doi: 10.1038/s41586-020-2797-4
202. Westein E, van der Meer AD, Kuijpers MJ, Frimat JP, van den Berg A, Heemskerk JW. Atherosclerotic geometries exacerbate pathological thrombus formation poststenosis in a von Willebrand factor-dependent manner. *Proc Natl Acad Sci USA*. 2013;110:1357–1362. doi: 10.1073/pnas.1209905110
203. Hulsmans M, Clauss S, Xiao L, Aguirre AD, King KR, Hanley A, Hucker WJ, Wülfers EM, Seemann G, Courties G, et al. Macrophages facilitate electrical conduction in the heart. *Cell*. 2017;169:510–522.e20. doi: 10.1016/j.cell.2017.03.050
204. McAleer CW, Pointon A, Long CJ, Brighton RL, Wilkin BD, Bridges LR, Narasimhan Sriram N, Fabre K, McDougall R, Muse VP, et al. On the

Downloaded from http://ahajournals.org by on March 22, 2021

potential of in vitro organ-chip models to define temporal pharmacokinetic-pharmacodynamic relationships. *Sci Rep*. 2019;9:9619. doi: 10.1038/s41598-019-45656-4

205. Mikryukov AA, Mazine A, Wei B, Yang D, Miao Y, Gu M, Keller GM. BMP10 signaling promotes the development of endocardial cells from human pluripotent stem cell-derived cardiovascular progenitors. *Cell Stem Cell*. 2021;28:96–111.e7. doi: 10.1016/j.stem.2020.10.003
206. van den Brink SC, Alemany A, van Batenburg V, Moris N, Blotenburg M, Vivié J, Baillie-Johnson P, Nichols J, Sonnen KF, Arias AM, et al. Single-cell and spatial transcriptomics reveal somitogenesis in gastruloids. *Nature*. 2020;582:405–409. doi: 10.1038/s41586-020-2024-3
207. van den Brink SC, Baillie-Johnson P, Balayo T, Hadjantonakis AK, Nowotschin S, Turner DA, Martinez Arias A. Symmetry breaking, germ layer specification and axial organisation in aggregates of mouse embryonic stem cells. *Development*. 2014;141:4231–4242. doi: 10.1242/dev.113001
208. Moris N, Anlas K, van den Brink SC, Alemany A, Schröder J, Ghimire S, Balayo T, van Oudenaarden A, Martinez Arias A. An in vitro model of early anteroposterior organization during human development. *Nature*. 2020;582:410–415. doi: 10.1038/s41586-020-2383-9
209. Piepoli MF, Hoes AW, Agewall S, Albus C, Brotons C, Catapano AL, Cooney MT, Corrà U, Cosyns B, Deaton C, et al; ESC Scientific Document Group. 2016 European guidelines on cardiovascular disease prevention in clinical practice: the sixth joint task force of the European Society of Cardiology and Other Societies on Cardiovascular Disease Prevention in Clinical Practice (constituted by representatives of 10 societies and by invited experts)Developed with the special contribution of the European Association for Cardiovascular Prevention & Rehabilitation (EACPR). *Eur Heart J*. 2016;37:2315–2381. doi: 10.1093/eurheartj/ehw106
210. Shinozawa T, Nakamura K, Shoji M, Morita M, Kimura M, Furukawa H, Ueda H, Shiramoto M, Matsuguma K, Kaji Y, et al. Recapitulation of clinical individual susceptibility to drug-induced QT prolongation in healthy subjects using iPSC-derived cardiomyocytes. *Stem Cell Reports*. 2017;8:226–234. doi: 10.1016/j.stemcr.2016.12.014
211. Kehat I, Gepstein A, Spira A, Itskovitz-Eldor J, Gepstein L. High-resolution electrophysiological assessment of human embryonic stem cell-derived cardiomyocytes: a novel in vitro model for the study of conduction. *Circ Res*. 2002;91:659–661. doi: 10.1161/01.res.0000039084.30342.9b

Downloaded from http://ahajournals.org by on March 22, 2021